nature medicine

Article

https://doi.org/10.1038/s41591-026-04314-9

Antisense oligonucleotide-mediated knockdown therapy in two infants with severe *KCNT1* epileptic encephalopathy

Received: 30 August 2024

Accepted: 26 February 2026

Published online: 14 April 2026

Check for updates

A list of authors and their affiliations appears at the end of the paper

KCNT1-related epileptic encephalopathy, including epilepsy of infancy with migrating focal seizures, is a severe neurodevelopmental disorder associated with refractory seizures, profound neurologic impairment and premature death. It is caused by de novo genetic variants in *KCNT1* that alter the function of Slack, an evolutionarily conserved sodium-gated potassium channel that modulates neuronal firing patterns and excitability. Pathogenic *KCNT1* variants lead to overactive Slack channels, boosting total neuronal potassium currents by up to 40%, driving cortical hyperexcitability and causing seizures. Here we investigate antisense oligonucleotide-mediated *KCNT1* knockdown as a therapeutic strategy for patients with epilepsy of infancy with migrating focal seizures. Intrathecal delivery of an experimental, non-allele-specific, *KCNT1*-targeting antisense oligonucleotide by lumbar puncture in two 2-year-old females with *KCNT1* p.R474H, a severe, recurrent pathogenic variant, led to a significant reduction in seizure frequency and intensity. However, investigational treatment was also associated with the development of ventricular enlargement or hydrocephalus in both patients, prompting in one case the redirection of goals of care, pointing to a potential monitorable toxicity of some intrathecal antisense oligonucleotides.

Epilepsy of infancy with migrating focal seizures (EIMFS, also referred to as *KCNT1*-related epileptic encephalopathy, early infantile 14 or EIEE14) is one of the most severe epilepsy syndromes[1–3]. Up to 50% of patients with EIMFS are found to have de novo pathogenic variants in *KCNT1* (refs. 2,4,5). *KCNT1* encodes a sodium-activated potassium channel (also referred to as Slack, SLO2.2 or $K_{Na}1.1$)[6–8] that is expressed widely in neurons throughout the central nervous system. Functional studies have shown that pathogenic *KCNT1* variants associated with epilepsy cause a gain of function in channel activity. In heterologous expression systems, *KCNT1* p.R474H, the most severe known human mutation, increases channel-mediated potassium currents up to 22-fold compared with the wild-type (WT) channel[4,6,9,10]. These overactive channels increase network hyperexcitability and have severe clinical consequences: affected individuals have refractory epilepsy with very frequent seizures, at times nearly continuous, global developmental delays and severe-to-profound intellectual disability. There are currently no effective treatments for this condition. Quinidine has been tried as a targeted therapy, but efficacy is inconsistent among patients, and it can be poorly tolerated owing to prolongation of the QT interval[11]. Patients with *KCNT1*-related EIMFS also have high early mortality, often related to seizure comorbidities or sudden unexpected death in epilepsy; nearly half of patients die before 3 years of age[1,2].

Antisense oligonucleotides (ASOs) are short chemically modified nucleic acids that can modify gene expression by either modulating mRNA splicing or triggering RNA degradation by recruiting ribonuclease H (RNase H), an endogenous nuclease that degrades the RNA

A full list of affiliations appears at the end of the paper

strand of RNA-DNA heteroduplexes. Examples of approved ASO drugs include nusinersen, a splice-modulating ASO designed to treat spinal muscular atrophy (SMA), and tofersen (BIIB067), an RNase H-activating ASO designed to treat *SOD1* amyotrophic lateral sclerosis (ALS)[12]. Investigational ASO therapies for orphan neurogenetic diseases have also been deployed in small-scale studies for single patients with severe, life-threatening conditions such as *CLN7* Batten disease, *FUS*-related ALS, *C9orf72*-related ALS, ataxia telangiectasia and *KIF1A*-associated neurologic disorder[13–16].

Here we report results of a translational investigation of the therapeutic impact of *KCNT1* knockdown with an RNase H-activating ASO in two patients with *KCNT1*-related EIMFS.

Results

Case histories

Two 2-year-old girls with neonatal-onset, treatment-refractory epilepsy and global developmental delay were each found to harbor a de novo *KCNT1* variant (c.1421G>A, p.Arg474His). Patient 1 developed seizures on day 4 of life (up to 20 daily), showed multifocal migrating discharges on the electroencephalogram (EEG), had normal brain magnetic resonance imaging (MRI) findings and failed trials of levetiracetam, topiramate, phenobarbital, diazepam, oxcarbazepine, valproic acid, quinidine, phenytoin and vitamin B_6; by 28 months, she showed severe axial hypotonia with poor head control; no rolling, reaching, fixation or hand-to-mouth movements; and variable appendicular tone. Patient 2 began having apneic spells with bicycling limb movements at 5 h of life (10–15 daily). The EEG showed multifocal migrating seizures, which were refractory to trials of phenobarbital, levetiracetam, pyridoxine, potassium bromide, phenytoin, cannabidiol and topiramate. At age 2, she showed diffuse hypotonia without head control, inability to roll, minimal visual tracking and fixation, and intermittent smile-like movements and could grasp but not hold objects (see Methods for more detailed information).

KCNT1-knockdown-ASO screening in cell lines and patient iPSC-derived neurons

ASO-mediated knockdown of mouse *Kcnt1* rescued seizures and early mortality in a mouse disease model without apparent deleterious consequences[17]. Furthermore, heterozygous loss-of-function variants in *KCNT1* are not significantly constrained in human population datasets (probability of loss-of-function intolerance, pLI = 0), supporting the potential clinical tolerability of reduction of gene dosage. To investigate this further, we designed a series of ASOs targeting human *KCNT1*.

We performed an in vitro screen to identify potent ASO sequences that reduced *KCNT1* expression. An overview of the screening cascade is shown in Fig. 1a. Potential ASO sequences tiling the human *KCNT1* mRNA sequence (NM_020822.3, 7,123 bp) were generated, using 5–10–5 gapmer designs (five 2′-*O*-(2-methoxyethyl) (2′MOE)-modified nucleotides, followed by ten unmodified nucleotides, followed by five 2′MOE-modified nucleotides) to trigger RNA transcript degradation by RNase H (ref. 18). Following ranking by bioinformatic properties (binding affinity, secondary structure, self-annealing and potential off-targets) and species cross-reactivity (prioritizing cross-reactivity to mice and/or rats), 263 sequences were selected for initial synthesis and testing. Of these, 12 were allele-selective designs Of these, 12 were allele-selective designs targeting the disease-associated variant (*rs53033*) or other linked single nucleotide polymorphisms (Fig. 1a and Supplementary Table 3). ASOs were tested first in human neuroblastoma cells (BE(2)-M17 and/or SH-SY5Y) that endogenously express *KCNT1*. Microwalking of promising candidates contributed 63 additional ASOs (32 allele specific and 31 allele nonspecific) for a second round of screening. Two more rounds of screening were conducted in patient-derived neuronal cells, evaluating 66 (58 allele specific, 8 allele nonspecific) and 30 (all allele nonspecific) additional designs, respectively, ultimately leading to the selection of four candidate leads: KT707ps, KT717ps, KT718ps and KT777ps (targeting exons 15, 11, 11 and the 7–8 junction, respectively; Fig. 1a and Extended Data Table 1). KT707ps overlapped the disease-causing *rs53033* (c.1421G>A) variant, rendering it potentially allele selective; KT717ps, KT718ps and KT777ps were allele-nonselective designs. In BE(2)-M17 cells treated with lipofection (100 nM), these candidates showed ~75% of knockdown of *KCNT1* levels (Fig. 1b and Extended Data Fig. 1a,b). Similar knockdown was observed in human induced pluripotent stem cell (iPSC)-derived neurons from patient 1 (Fig. 1c) or an unrelated donor (Extended Data Fig. 1c). KT707ps showed a half maximal inhibitory concentration (IC_{50}) of 28.28 nM and only modest allele selectivity (~80% knockdown in patient-derived neurons versus ~60% knockdown in the WT; Fig. 1c and Extended Data Fig. 1c,d). KT777, a derivative of KT777ps with the same sequence but reduced PS content (that is, using a mixed phosphodiester and phosphorothioate backbone), showed further improvement in potency in patient-derived neurons (IC_{50} 0.64 nM; Fig. 1d and Extended Data Fig. 1d). Finally, we tested our leads via gymnosis (free uptake from the media), mimicking in vivo uptake[19]. Among our candidates, KT777 and KT777ps showed the highest efficacy in BE(2)-M17 cells and patient-derived neurons, with durable *KCNT1* mRNA and protein reduction for 2 weeks (Fig. 1e,f and Extended Data Fig. 1e,f), supporting their advancement as our top two clinical candidates.

Off-target binding potential was assessed computationally and experimentally. In silico analyses revealed no full-length matches of KT777/KT777ps in the spliced or pre-spliced human transcriptome (allowing for up to two mispairings). A limited number of potential off-targets (with two mispairings) were predicted after allowing for 5′/3′ trimming of one nucleotide (Extended Data Table 2). We used RNA sequencing (RNA-seq) to perform transcriptome-wide analysis of gene expression patterns in human iPSC-derived neurons before and after gymnotic treatment and found none of these potential targets to be significantly perturbed by KT777 (Fig. 1g and Supplementary Tables 4 and 5). Overall selectivity of KT777 knockdown (*KCNT1* downregulated at an adjusted *P* value (P_{adj}) = 1.7×10^{-34}; 11 additional downregulated genes nominally significant at $P_{adj} < 0.05$; Supplementary Table 5) was similar to that of RNase H-activating ASOs BIIB067 and HTTRx (targeting *SOD1* and *HTT*, respectively) (Supplementary Figs. 1 and 2). Of 36 genes in the Action Potential biological process (GO_0001508), *KCNT1* was the only gene to be significantly affected (Supplementary Table 6). Pathway analysis showed no overall changes in the expression of specific biological pathways in response to KT777 treatment (Supplementary Tables 5 and 6).

Impact of *KCNT1* reduction on electrophysiologic currents

iPSC-derived neurons from patients with *KCNT1*-related epilepsy show elevated total outward potassium (K^+) currents compared with isogenic controls[8]. We therefore examined the impact of *KCNT1* knockdown on total outward potassium (K^+) currents. We first performed whole-cell voltage-clamp recordings on patient iPSC-derived neurons bearing the h*KCNT1* p.R474H variant. Treatment with *KCNT1*-targeting ASOs (KT777 or KT717ps) suppressed total outward K^+ currents in patient neurons, compared with neurons treated with a non-targeting control ASO (Fig. 2a–c and Extended Data Fig. 2a–d). Current-clamp recordings showed that *KCNT1* p.R474H neurons exhibited increased action potential (AP) firing rates, increased amplitudes and relatively narrower AP half widths; these effects were reversed by KT777 ASO treatment (Fig. 2d,e), supporting the notion that knockdown of *KCNT1* could reverse the hyperexcitability of these neurons. Patient neurons treated with ASOs for up to 3 weeks appeared healthy and showed normal neurite morphology, suggesting that long-term modulation of these pathologic electrophysiological abnormalities by KT777 could be tolerated at the cellular level (Extended Data Fig. 2e–g).

The target sequence of KT777/KT777ps is conserved between human *KCNT1* and mouse *Kcnt1*, allowing us to test its impact in this animal model. In mouse Neuro2a neuroblastoma cell lines,

https://doi.org/10.1038/s41591-026-04314-9

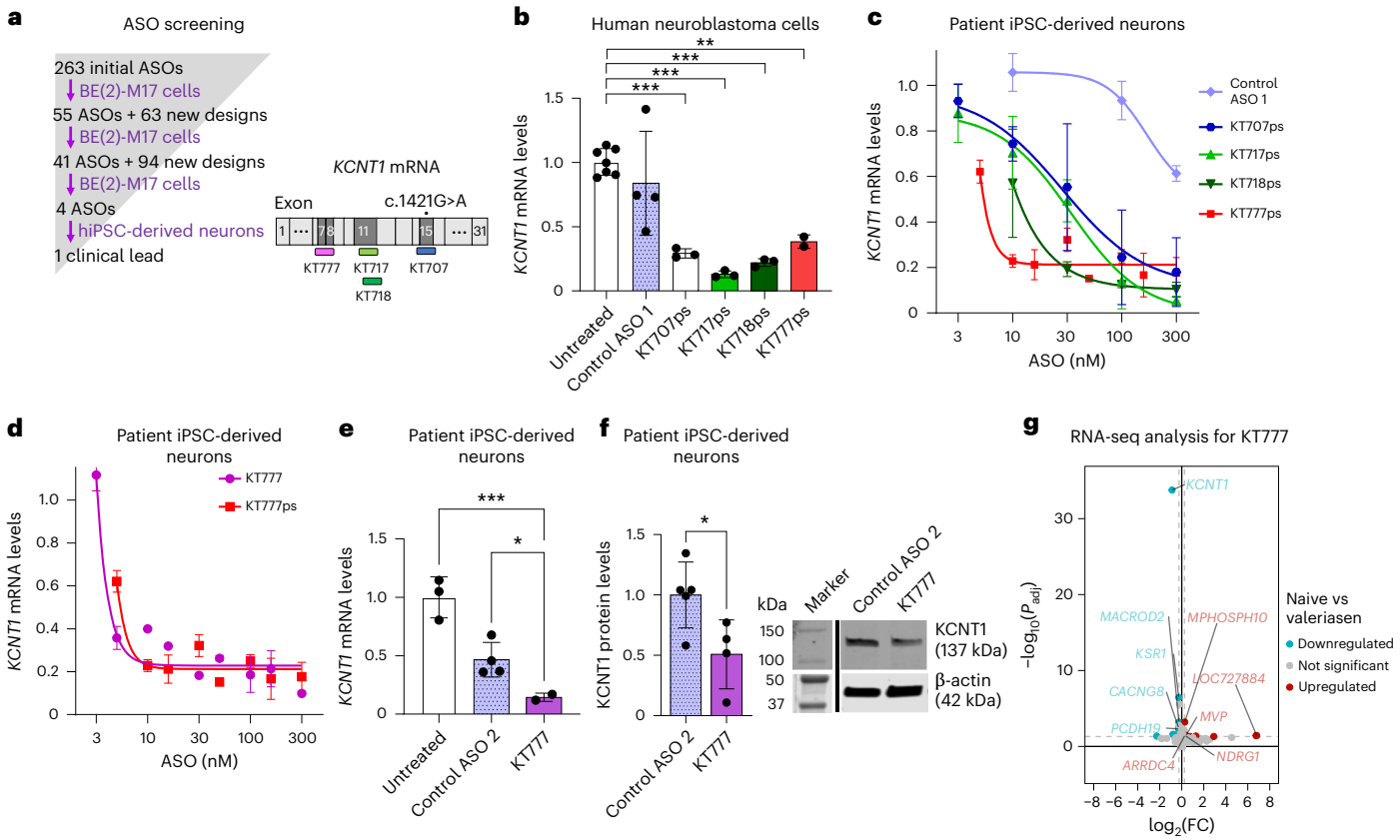

Fig. 1 | 2′MOE-modified ASOs reduce *KCNT1* transcripts in patient iPSC-derived neurons. a, ASO development process and candidate leads mapped on a *KCNT1* mRNA transcript. Iterative screening, concentration-response curve studies and in vivo evaluations yielded the final clinical lead ASO. KT717/KT717ps, KT718/KT718ps and KT777/KT777ps are non-allele-specific ASOs targeting sequences in exon 11, exon 11 and the exon 7–8 junction, respectively. KT707 was an allele-specific ASO designed to overlap and preferentially bind the mutant c.1421G>A allele. ASO sequences and control ASOs are shown in Extended Data Table 1. Tested sequences included versions with full phosphorothioate backbones (for example, KT707ps, KT717ps, KT718ps, KT777ps) and versions with mixed phosphorothioate and phosphodiester backbones (for example, KT707, KT717, KT718, KT777). **b**, Initial ASO screens in human neuroblastoma cells (BE(2)-M17 cells) via lipofection at 100 nM. Treatment groups (KT707ps, $n = 3$; KT717ps, $n = 3$; KT718ps, $n = 3$; KT777ps $n = 2$) significantly reduced *KCNT1* mRNA levels compared with untreated samples (untreated versus KT707ps, $P = 0.0005$; untreated versus KT717ps, $P < 0.0001$; untreated versus KT718ps, $P = 0.0002$; untreated versus KT777ps, $P = 0.0081$). No significant differences were observed among the four treatment groups (untreated, $n = 7$; control ASO1, $n = 4$). **c**, Initial ASO screens in patient iPSC-derived neurons via lipofection ($n = 2$ for control, KT718ps, KT777ps; $n = 4$ for KT717ps; $n = 1$ for KT707). **d**, Dose–response curves in patient iPSC neurons via lipofection for KT777 (mixed phosphodiester and phosphorothioate backbone; purple) and KT777ps (full phosphorothioate backbone; red) ($n = 2$ except $n = 1$ for KT777 at 10–300-nM doses). **e**,**f**, Characterization of effects of lead ASO (KT777) administration to patient iPSC-derived neurons via 2 weeks of treatment at 10 µM by gymnotic delivery, showing significant decreases in *KCNT1* mRNA levels (untreated, $n = 3$; control ASO 2, $n = 4$; KT777, $n = 2$; untreated versus KT777, $P = 0.0006$; KT777 versus control ASO 2, $P = 0.0347$) (**e**) and KCNT1 protein levels (control ASO 2, $n = 5$; KT777, $n = 4$; control ASO 2 versus KT777, $P = 0.0337$) (**f**). **g**, Volcano plot of differential gene expression in naive versus KT777-treated human neurons treated via gymnosis at DIV 22 and collected at DIV 29. Dashed lines indicate significance thresholds ($P_{adj} \leq 0.05$, $\log_2(FC) > |0.25|$); significantly upregulated and downregulated genes are indicated;the top five significantly upregulated and downregulated genes are labeled (Wald test P value, Benjamini–Hochberg adjusted). In **b**–**f**, results represent the mean with s.d., two to six biological replicates per experiment and one or two technical replicates per biological replicate. In all panels, $^*P < 0.05$, $^{**}P < 0.01$ and $^{***}P < 0.001$ (one-way ANOVA with Dunnett's multiple comparisons test in **b** and **e**; two-tailed unpaired t-test in **f**).

KT777ps suppressed *Kcnt1* expression with an IC_{50} of 13.4 nM (Extended Data Fig. 3a). We also performed voltage-clamp recordings from mouse cortical neurons harboring *Kcnt1* p.R455H, the mouse ortholog of the pathogenic human *KCNT1* p.R474H variant. Gymnotic treatment of heterozygous p.R455H neurons with KT777 (Fig. 2f–h and Extended Data Fig. 4a–d) resulted in the normalization of outward currents back to levels measured from isogenic controls. Collectively, these results lent support to the hypothesis that ASO knockdown of *KCNT1* by KT777 or KT777ps could ameliorate the pathological neuronal electrophysiologic abnormalities associated with *KCNT1* p.R474H.

In vivo rodent studies

To evaluate the in vivo impact of our lead *KCNT1*-targeting ASOs, we performed intracerebroventricular (ICV) injection of KT777ps into WT mice. ICV injection of 25 µg, 75 µg or 200 µg KT777ps elicited dose-dependent reductions in *Kcnt1* mRNA in the cortex, hippocampus and spinal cord at 14 days postinjection (Extended Data Fig. 3b). ICV injections of KT777ps and KT777 also led to dose-dependent reductions in *KCNT1* mRNA in the brains of transgenic mice engineered to express both native mouse *Kcnt1* and human *KCNT1* (Fig. 3a,b and Extended Data Fig. 3c,d). Intrathecal (IT) injections of 800 µg KT777 also induced up to 70% reductions in *Kcnt1* mRNA levels in rat brain tissue, confirming in vivo target engagement (Fig. 3c,d, Extended Data Fig. 3e–l and Supplementary Table 7).

We tested KT777ps in the *Kcnt1 P905L*$^{(L/L)}$ mouse. This is a previously established model of *KCNT1*-related epilepsy[17] that shows severe neurocognitive defects and spontaneous seizures; these mice are also prone to status epilepticus and have a median lifespan of 44 days. A total of 16 *Kcnt1 P905L*$^{(L/L)}$ mice received KT777ps (100 µg, ICV), with 5 mice receiving a single dose at P31–35 and 11 mice receiving 2 doses

at P31–35 and P149–164. KT777ps treatment resulted in a significant and dose-responsive improvement in lifespan, with median survival increased to 133 days after a single dose (range 1–169 days postinjection) and further extended to 233.5 days following 2 doses (Fig. 3e). Injection of a single dose of KT777ps into day 40–49 *Kcnt1 P905L*$^{(L/L)}$ mice also rescued neurocognitive defects, with nest building scores of 1.1 in untreated *P905L*$^{(L/L)}$ mice before treatment, 4–5 for WT mice and 4.4 in *P905L*$^{(L/L)}$ mice 2 weeks after KT777ps treatment (Fig. 3f).

Safety characterization and IND-enabling studies

Considering the poor prognosis of children with *KCNT1* p.R474H EIMFS and evidence of phenotypic rescue in human in vitro neuronal and mouse disease models, we initiated Investigational New Drug (IND)-enabling studies for potential clinical investigational use. At very high doses, IT administration of ASOs can cause transient motor phenotypes ranging from reduced motor activity to acute ataxia to acute seizure-like phenotypes[20–23]. To screen for these, we manufactured clinical-grade KT777 and KT777ps (and the backup candidate KT718) and tested them via IT dosing in Sprague Dawley rats. In early lead prioritization studies, at 2 mg per dose, KT777ps and KT718 elicited high incidences of seizures and behavioral abnormalities, excluding them from further development. By contrast, animals receiving 1 mg or 2 mg IT doses of KT777 showed only transient limited hindlimb usage (1/5 and 5/5 animals at 1 mg and 2 mg, respectively) and hypoactivity (1/5 and 1/5 animals at 1 mg and 2 mg, respectively) at 3 h, with symptoms resolving by 24 h. Injections of 0.2 mg elicited no abnormal clinical signs, with functional observation battery parameters comparable to those of controls.

Repeat-dose injections (days 1, 15, 29, 43 and 99) of 0 mg, 0.05 mg, 0.2 mg or 0.8 mg KT777, performed under Good Laboratory Practices (GLP) guidelines, showed that up to 0.8 mg per dose was well tolerated over 15 weeks (in-life measures including cage side observations, functional observation batteries). Comprehensive neuropathologic assessment of animals killed on day 115 or day 155 showed only minimal, nonprogressive findings of macrophage and neuronal vacuolation, and nerve-fiber degeneration (see Methods and 'Detailed Rat Preclinical Studies' in the Supplementary Information for details).

Clinical trial and initial responses in patients 1 and 2

On the basis of these results, we designed an investigational clinical protocol incorporating stepwise IT KT777 (renamed 'valeriasen') escalation, seizure monitoring and neurodevelopmental outcomes (Fig. 4a and Extended Data Fig. 5). Permission to proceed was granted in July 2020 (IND 147092). A first patient with *KCNT1* p.R474H EIMFS began dosing in September 2020, and a second patient began dosing in June 2021 (Extended Data Fig. 6a).

Patient 1 was 3 years old at the time of the study initiation. She received escalating IT doses of 10 mg, 20 mg, 30 mg and 40 mg of valeriasen via lumbar puncture on weeks 0, 2, 4 and 6. This was followed by maintenance dosing of 40 mg every 8 weeks beginning at week 10 (Fig. 4a). Maintenance dosing increased to 60 mg every 8 weeks at week 26. Over the course of the study, the patient showed improvement in observed seizure frequency and severity (Fig. 4b,e and Extended Data Fig. 7a) compared with the pretreatment baseline, corroborated by an EEG review (Table 1). The EEG background of patient 1 during wakefulness consisted of diffuse, generalized slowing with frequent multifocal spikes and a suppression burst pattern during sleep. No major changes in background patterns were observed over the course of the trial.

Patient 2 was enrolled 9 months later and was 3 years old at the time of study initiation. She received escalating IT doses of 10 mg, 20 mg, 30 mg and 40 mg (Fig. 4c). Seizure frequency began to decline after her 20 mg dose and more significantly after the 30 mg dose. During this period, her family also reported a variety of positive neurocognitive changes at home, including improved head control, swallowing and self-soothing by chewing on her fingers. Immediately before her fourth dose, video EEGs documented a 50% seizure reduction from baseline. After her fourth dose, seizure frequency dropped to 0–3 per day for nearly 50 days (Fig. 4c,f). Video EEGs documented a decline in seizures from 10–22 per day to 4 per day (Table 1). Like patient 1, the EEG background of patient 2 did not change significantly over time, with diffuse, generalized slowing with frequent multifocal spikes during wakefulness and a suppression burst pattern during sleep.

Trough cerebrospinal fluid (CSF) and plasma drug levels and plasma postinjection drug levels for patients 1 and 2 are shown in Extended Data Figs. 7b,c and 8a,b.

Safety and adverse events

Over the study's first 10 months, CSF and blood safety lab results were unremarkable (Extended Data Fig. 8c,d and Supplementary Table 8). Quantitative sensory testing studies[9,24] showed no significant changes in mechanical detection thresholds or pain thresholds.

Between the 4th and 5th dose (weeks 8–12), patient 1 developed dystonia, which was noticed on her exam before the 5th dose (Extended Data Fig. 6b). This was reported as a serious adverse event of uncertain correlation with the investigational therapy, given that dystonia and status dystonicus is sometimes part of the *KCNT1*-related epilepsy phenotype[25]. She was evaluated by movement disorder, physiatry

Fig. 2 | Lead ASO KT777 ameliorates firing patterns and K^+ currents in mutant iPSC-derived neurons and mouse cortical neurons. a–**c**, Voltage-clamp recordings of iPSC-derived neurons of WT and patient iPSC-derived neurons. Representative traces of steady-state outward currents (**a**), averaged currents (**b**) and current at 50 mV (**c**) of WT cells (black, $n = 11$), untreated R474H patient cells (red, $n = 6$), R474H patient cells treated with a control ASO (blue, $n = 5$) and R474H patient cells treated with lead ASO KT777 (purple, $n = 5$). Outward currents measured in patient iPSC-derived neurons were larger than those measured from WT cells. Gymnotic treatment with KT777, but not control ASOs, reduced outward currents in patient iPSC-derived neurons, a level comparable to that of the WT (WT versus R474H, $P = 0.0074$; R474H versus R474H + KT777, $P = 0.0025$). **d**, Changes in AP in iPSC-derived neurons with lead ASO treatment. Representative AP traces in response to a depolarizing current step stimulus during current-clamp recordings show that R474H patient-derived neurons (red) have more frequent APs of higher amplitude than WT cells (black). Treating patient cells with lead ASO KT777 (purple) reduced the firing frequency compared with either untreated patient cells (red) or patient cells treated with the control ASO (blue). **e**, R474H patient cells treated with lead ASO (purple, $n = 4$) showed reduced AP amplitude (WT versus R474H, $P = 0.0441$; R474H versus R474H + KT777, $P = 0.0157$), reduced maximal number of APs (WT versus R474H, $P = 0.0161$; R474H versus R474H + KT777, $P = 0.0293$) and increased AP half width (R474H versus R474H + KT777, $P = 0.0463$) compared with untreated (red, $n = 8$) or control-treated patient cells (blue, $n = 4$). No changes in AP afterhyperpolarizations (AHP) were found. WT $n = 10$. Max, maximum. **f**–**h**, Voltage-clamp recordings of E16–17 embryonic cortical neurons isolated from WT and R455H mutant mice and treated with lead ASOs. Representative traces of steady-state outward currents (**f**), averaged currents (**g**) and current at 50 mV (**h**) are shown. Mouse cortical neurons from WT mice (WT/WT), heterozygous p.R455H mice (R455H/WT) and homozygous p.R455H mice (R455H/R455H) were treated with control ASO and KT777. Heterozygous R455H cortical neurons treated with lead ASO KT777 showed significant steady-state outward current reduction compared with heterozygous R455H treated with control ASO (R455H/WT + control ASO 2 versus WT + control ASO 2, $P = 0.0132$; R455H/WT + control ASO 2 versus R455H/R455H + control ASO 2, $P < 0.0001$; R455H/WT + control ASO 2 versus R455H/WT + KT777, $P = 0.0153$). WT/WT + control ASO $n = 17$, R455H/WT + control ASO $n = 16$, R455H/R455H + control ASO and R455H/WT + KT777 $n = 15$. In **b**, **c** and **e**, $n = 4$–13 neurons per condition from 4 coverslips across 2 independent differentiations. In **g** and **h**, $n = 15$–17 neurons per condition from 3 independent cultures derived from 3 pregnant mice. Data are presented as mean values ± s.e.m. $^*P < 0.05$, $^{**}P < 0.01$ and $^{***}P < 0.001$, comparing treatment groups from samples tested by control ASOs (one-way ANOVA with Dunnett's multiple comparisons test).

https://doi.org/10.1038/s41591-026-04314-9

and physical therapy specialists and treated for status dystonicus with a course of clonazepam, baclofen and gabapentin, and improved.

Patient 1 developed vomiting and apparent discomfort, specifically in a moving vehicle, 8 weeks after her 9th IT dose. Brain and spine imaging was obtained 2 days later and revealed severe communicating hydrocephalus with T2 white matter changes representing transependymal flow but no other parenchymal changes. On exam, she was at her baseline level of alertness and did not show obvious signs of discomfort. Her tone was mildly increased from baseline. Her pupils were equal and reactive, extraocular movements were normal without evidence of the sunset eye sign, and heart rate and blood pressure were normal. An endoscopic third ventriculostomy with choroid plexus cauterization was performed, showing a CSF opening pressure of 55 cm H_2O. No improvement in hydrocephalus was seen over the following 2 days. After considering ventriculoperitoneal shunt placement, and mindful of the seriousness of her disease course before experimental

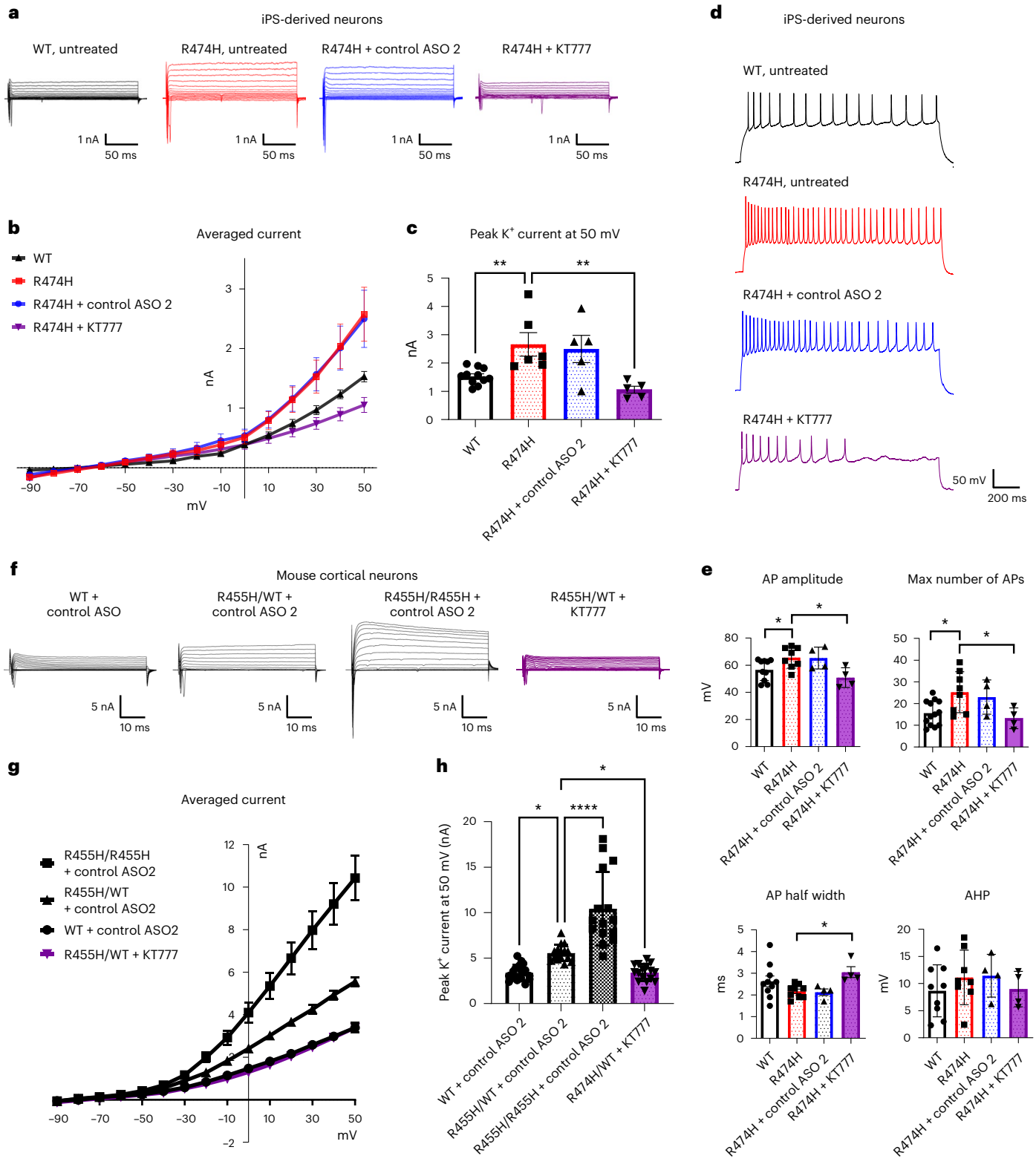

https://doi.org/10.1038/s41591-026-04314-9

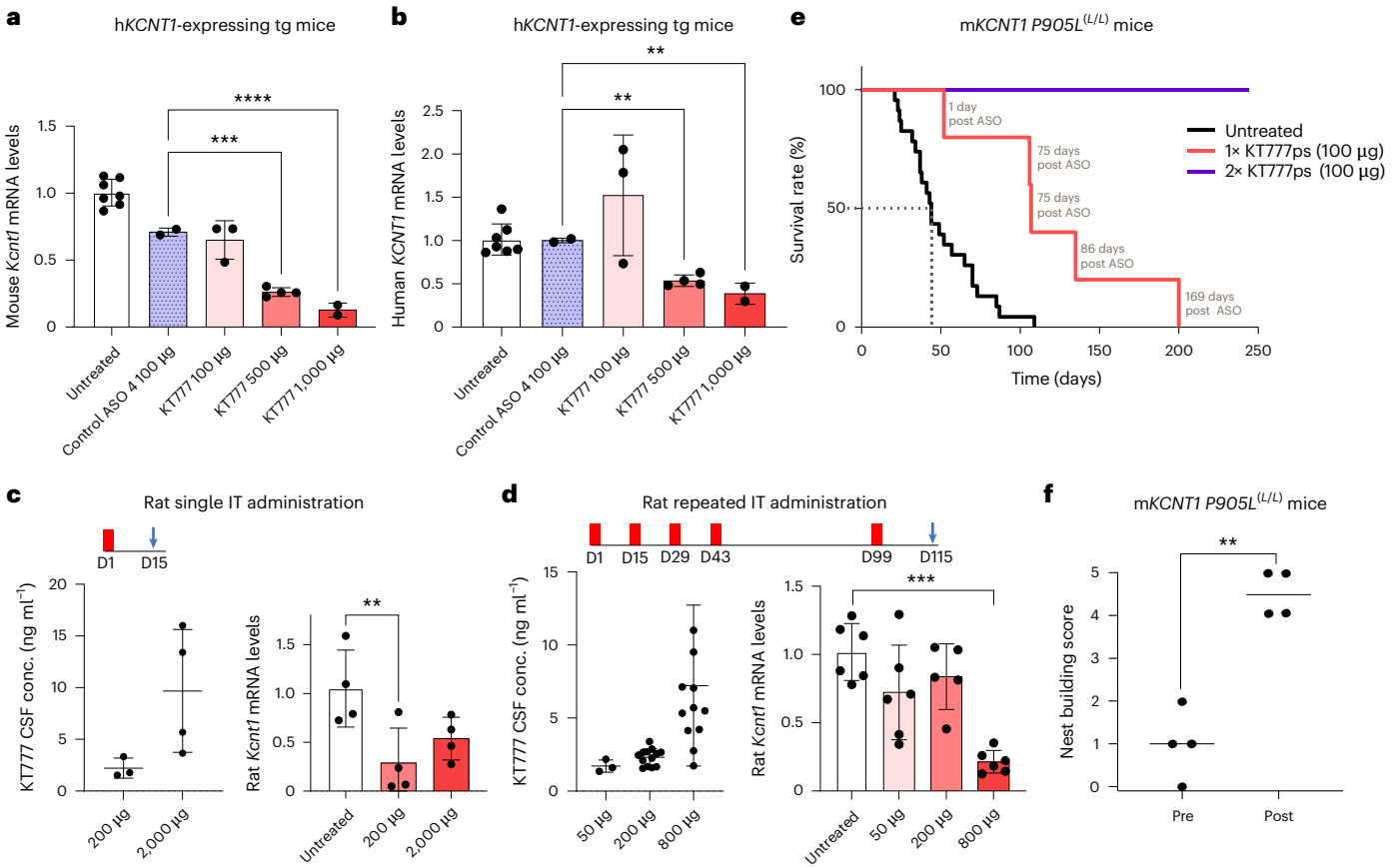

Fig. 3 | Treatment with lead ASO KT777 reduces *KCNT1* levels and improves life expectancy and neurocognitive defects of *Kcnt1 P905L*$^{(L/L)}$ mice. **a**,**b**, Measurement of levels of mouse *Kcnt1* (**a**) or human *KCNT1* (**b**) in the cortex of human *KCNT1* (h*KCNT1*)-expressing mice, 10–11 days after injection with vehicle (untreated), control ASO and KT777. Asterisks denote significant changes from the ASO control (control ASO 4 100 µg versus KT777 500 µg, $P = 0.0003$, and control ASO 4 100 µg versus KT777 1,000 µg, $P \leq 0.0001$, in **a**; control ASO 4 100 µg versus KT777 500 µg, $P = 0.0077$, and control ASO 4 100 µg versus KT777 1,000 µg, $P = 0.0031$, in **b**). Untreated $n = 7$; control ASO 100 µg $n = 2$; KT777 100 µg $n = 3$, 500 µg $n = 4$ and 1,000 µg $n = 2$. **c**,**d**, IT administration of KT777 in WT rats. Injection protocols are shown at the top with dosing days (red bars) and analysis points (blue arrows). Single administration of KT777 at 200 µg and 2,000 µg (**c**) elicits reduction of *Kcnt1* levels in the rat frontal cortex at 14 days postinjection (untreated versus 200 µg $P = 0.0184$). KT777 was robustly detected in CSF 14 days after dose. $n = 4$ except for $n = 3$ for KT777 CSF concentration at 200 µg. Repeat dosing of KT777 at 800 µg (**d**) leads to a significant decrease of *Kcnt1* in the rat frontal cortex at 115 days (untreated versus 800 µg, $P < 0.0001$). Untreated $n = 6$, 50 µg $n = 6$, 200 µg $n = 5$ and 800 µg $n = 6$. KT777 was detected in a dose-dependent manner in CSF. 50 µg $n = 3$, 200 µg $n = 13$ and 800 µg $n = 12$. **e**, Treatment with KT777ps improves life expectancy in *Kcnt1 P905L*$^{(L/L)}$ mice. *P905L*$^{(L/L)}$ mice were dosed with KT777ps at 100 µg once (1× KT777ps, $n = 5$) or twice (2× KT777ps, $n = 11$). Times of dosing were P31–35 for the first dose and P149–164 for the second dose. Four mice not recovering from the first administration surgery were excluded. Five mice that received a single dose of KT777ps died at 1 day, 75 days, 75 days, 86 days and 169 days postinjection, respectively. The survival curve of untreated mice was obtained from previous data[17]. **f**, Nest building scores of *Kcnt1 P905L*$^{(L/L)}$ mice improved after treatment with KT777ps (100 µg ICV, 'Post', $n = 4$) compared with the untreated condition ('Pre', $n = 4$). Symbols are 48-h values after the initiation of the nest-building experiment for each mouse. Four mice that survived until 2 weeks after administration of KT777ps were reassessed for nest building. The mean nest building score after treatment was significantly improved from the untreated condition ($P < 0.01$). Horizontal lines represent the mean for each group ($n = 4$). For panels **a**–**d**, data are presented as mean values ± s.e.m. *$P < 0.05$, **$P < 0.01$ and ***$P < 0.001$, comparing treatment groups from samples tested by control ASOs or untreated samples (one-way ANOVA with Dunnett's multiple comparisons test). For panel **f**, data are presented as mean values. **$P < 0.01$, from the pretreatment baseline (two-tailed Mann–Whitney *U* test). tg, transgenic; conc., concentration; D, day.

therapy, the family withdrew from the investigational protocol in favor of palliative care. She subsequently died under hospice care, 3 months after the final ASO dose (Extended Data Fig. 6b).

Patient 2 entered the investigational protocol ~2 months before the detection of hydrocephalus in patient 1 (Extended Data Fig. 6a,c). No significant adverse events were noted for patient 2 through the first three doses (10 mg, 20 mg and 30 mg). A few days after her 40 mg dose, she developed increased muscle tone accompanied by intermittently sustained upward eye movement, suggestive of dystonia. Plasma CPK levels were within normal limits. A brain MRI was unremarkable (including normal ventricular size) (day 55). Lumbar puncture showed a normal opening pressure of 16 cm H_2O. CSF WBCs and protein were slightly elevated at 28 cells mm^{-3} and 83 mg dl^{-1}, respectively (and follow-up cell counts and protein levels were normal) (Supplementary Table 8). She was diagnosed with status dystonicus, like patient 1, and treated with hydration and trials of diphenhydramine, benzodiazepines, baclofen, carbidopa–levodopa and trihexyphenidyl, with gradual improvement to baseline. Plasma CPK rose to 5,794 U l^{-1} within 2 days and then normalized over several days. While the initial brain MRI (day 55) had been unremarkable, repeat MRIs performed on days 62 and 64 showed mild increases in ventricular size. There was no evidence of obstruction. Given the hydrocephalus found in patient 1, patient 2 was transferred to the pediatric intensive care unit for closer neurologic monitoring, where an extraventricular drain was placed. Opening pressure was >20 cm H_2O. There was persistent drainage through the extraventricular drain, and a ventriculoperitoneal shunt was placed on day 65. Ventricular dilatation gradually normalized on serial MR ventriculograms, and she was discharged to home in stable condition

https://doi.org/10.1038/s41591-026-04314-9

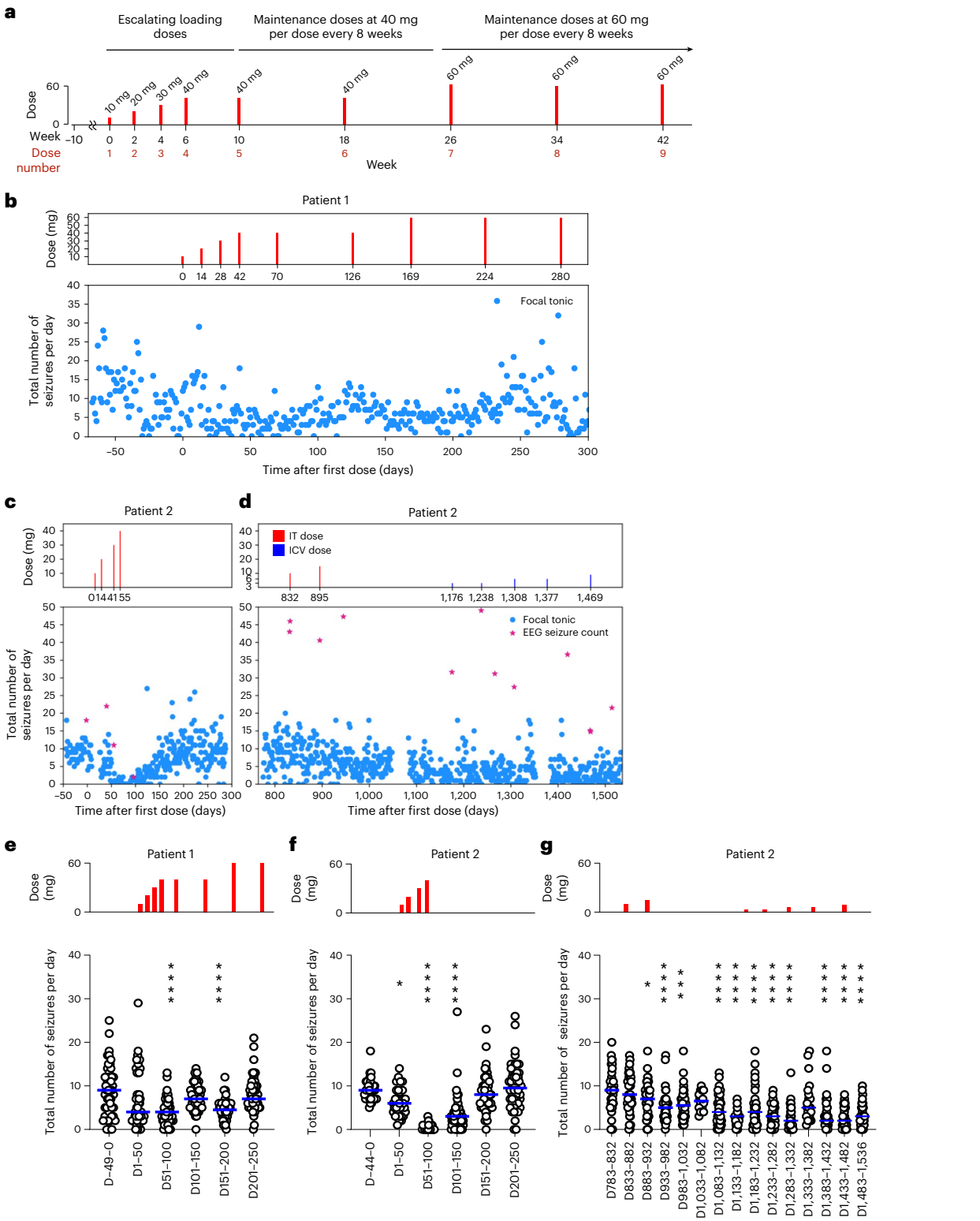

Fig. 4 | Clinical trials of two patients with EIMFS with valeriasen. a, Dosing schedule. **b**–**d**, Trends in seizure frequency and duration in patient 1 (**b**) and patient 2 (**c**, **d**) as reported in seizure diaries recorded by the parents. Actual dosing is indicated by red bars. The total number of focal tonic seizures per day was counted. In patient 1, we started to count myoclonic seizures (subtle body movement lasting less than 1 s) from day 241. **e**–**g**, Daily seizure counts and binned averages for every 50-day period before and after dosing in patient 1 (**e**) and patient 2 (**f**, **g**). In patient 2, dosing was resumed on day 832. Actual dosing is indicated by red bars. Seizure frequency was significantly reduced after valeriasen treatment (****$P < 0.0001$; D −44 to 0 versus D1–50 $P = 0.0109$ in **f**; D783–832 versus D883–932 $P = 0.0370$ and D783–832 versus D983–1,032 $P = 0.0002$ in **g**). $n = 50$ in **e**. D −44 to 0 $n = 38$, D1–50 $n = 33$, D51–100 $n = 39$ and others $n = 50$ in **f**. D1,033–1,082 $n = 16$, D1,133–1,182 $n = 43$, D1,183–1,232 $n = 46$, D1,383–1,432 and D1,433–1,482 $n = 48$, D1,483–1,536 $n = 54$ and others $n = 50$ in **g**. Data are presented as mean values. In **e**–**g**, *$P < 0.05$, ***$P < 0.001$ and ****$P < 0.0001$; all significance is compared with the leftmost column in each figure (one-way ANOVA with Dunnett's multiple comparisons test). Detailed seizure trends by seizure semiology and seizure duration are described in Extended Data Fig. 7a. The seizure type in patient 2 is focal tonic seizures with or without secondary generalized clonic seizures.

https://doi.org/10.1038/s41591-026-04314-9

Table 1 | EEG analysis of patients with KT777 treatment

EEG date	Seizures (normalized to 24 h)	Duration	Semiologies
Patient 1			
Week 0	19	15–60 s	Focal tonic
Week 5	17	15–90 s	Focal tonic, ± progression into unilateral clonic
Week 23	18	1–64 s (tonic), <1 s (myoclonic)	Majority focal tonic (17), minority myoclonic (1)
Week 29	33	10–30 s (tonic), <1 s (myoclonic)	Majority focal tonic (30), minority myoclonic (3)
Week 36	30	10–30 s (tonic), <1 s (myoclonic)	Majority myoclonic, minority brief focal tonic[a]
Week 45	20	10–30 s (tonic), <1 s (myoclonic)	Majority brief focal tonic (19), minority myoclonic (1)
Patient 2			
Week 0	18	6–10 s	Focal tonic
Week 4	22	8–15 s	Focal tonic
Week 6	10	9–22 s	Focal tonic
Week 14	4	12–40 s	Focal tonic

[a]Seizure count by semiology for patient 1 week 36 is not available.

on day 87 (Extended Data Fig. 6c). Adverse events for both patients are summarized in Supplementary Tables 9 and 10.

Investigational dosing was paused. Seizure frequency gradually returned to pretreatment baselines (Fig. 4c,f). CSF testing was negative for inflammatory biomarkers (albumin, IgG index, oligoclonal bands and neoptyrin), and neurologic surveillance with serial clinical examinations revealed no evolution of additional signs or symptoms. A review of preclinical and clinical findings led to our working hypothesis that hydrocephalus was a dose-related clinical side effect (Discussion). A revised protocol was developed, using lower doses, periodic MRI ventriculograms and opening pressure measurements with each lumbar puncture. ASO administration for patient 2 resumed after a 2-year hiatus. Two IT doses (10 mg and 15 mg, spaced 2 months apart) and five ICV doses (3 mg, 3 mg, 6 mg, 6 mg, 9 mg, spaced 2 months apart) were safely delivered, with a reduction in seizures of ~66% to date (Fig. 4d,g).

Discussion

The recognition of epilepsy's strong genetic basis, with well over 100 monogenic causes now identified[26,27], has revolutionized our understanding of epilepsy's mechanistic basis and has led to the expectation that this knowledge could lead to novel clinical therapies[28]. In this study, we explored the therapeutic potential of ASOs designed to inhibit *KCNT1* expression[29], a gene associated with severe neurodevelopmental epileptic encephalopathy via toxic gain-of-function mutations. Epilepsy-associated mutations in the Slack channel alter channel electrophysiologic properties, greatly magnifying sodium-gated potassium flux and potentially having other cellular effects as well[6], motivating a therapeutic strategy focusing on reducing levels of the pathogenic protein with knockdown ASOs. Promising results from ASO therapy (which requires intermittent redosing) could also validate *KCNT1* as a target for potential future long-term treatments, such as virally delivered Clustered Regularly Interspaced Short Palindromic Repeats (CRISPR) gene editing.

Here we show that a non-allele-selective ASO targeting human *KCNT1* reduced *KCNT1* mRNA levels, suppressed elevated potassium currents and reversed abnormally elevated AP firing rates in iPSC-derived neurons from patients with *KCNT1* p.R474H-associated EIMFS. This same ASO rescued potassium current, neurobehavioral, seizure and lifespan defects in mouse disease models, reinforcing previous findings with ASO-mediated *Kcnt1* knockdown in mice[17]. Furthermore, two patients with *KCNT1* p.R474H-associated EIMFS received an intrathecally delivered *KCNT1*-targeting ASO and showed signs of seizure improvement based on both caregiver diaries and interval EEGs.

Despite seizure improvements, both patients also developed hydrocephalus. Patients with early-onset *KCNT1*-related epilepsy commonly develop cortical atrophy, which can lead to ex vacuo ventricular size increases, but frank hydrocephalus with increased intracranial pressure is not expected[30]. Furthermore, hydrocephalus was not observed in *Kcnt1* knockout mice or knock-in mice expressing the *Kcnt1* R455H mutation[31].

We therefore considered the serious adverse events encountered in our two patients to be attributable to dosing of the study drug. We formally considered whether this side effect might represent (1) an on-target effect (that is, a consequence of *KCNT1* target modulation) or (2) an off-target effect of this sequence, or of high-dose IT ASOs in general[32].

With respect to possible on-target effects, human *KCNT1* is broadly expressed throughout the central nervous system, including the choroid plexus[33] (responsible for producing CSF) and arachnoid granulations[28] (responsible for CSF reabsorption). Its function in these regions is unclear, but it is conceivable that the reduction of *KCNT1* levels might potentially impact the electrolyte–fluid balance or tissue physiology. Partially arguing against this, complete genetic ablation of mouse *Kcnt1* is not known to exhibit a ventricular phenotype[7].

With respect to possible off-target effects, in silico and experimental analyses did not reveal evidence of significant off-target gene downregulation at sequence-related sites. Overall specificity of valeriasen's effects appeared similar to other knockdown ASO sequences in clinical use. Regarding potential class effects, studies in animals have linked CNS delivery of ASOs to acute neurobehavioral changes[22] and dorsal root ganglion injury, but ventricular enlargement or hydrocephalus has not been reported. Clinically, five patients with SMA treated with the IT ASO nusinersen have been reported in the literature to have hydrocephalus[34–36], but causation has not been established, and historical data suggest that patients with SMA may have an elevated risk of hydrocephalus[37] at baseline. Papilledema and increased intracranial pressure have been reported as rare potential side effects in patients with ALS treated with tofersen. Ventricular enlargement or hydrocephalus was also reported in adults with Huntington's disease receiving high doses (120 mg every 4 weeks or 8 weeks) of tominersen, an intrathecally delivered, RNase H-activating knockdown ASO that uses the same pattern and type of nucleotide and backbone modifications[38,39] as valeriasen. These doses were comparable to the dose exposures in our trial participants who developed hydrocephalus (for example, 10 mg + 20 mg + 30 mg + 40 mg = 100 mg delivered over the first 6 weeks for our second patient). However, hydrocephalus or ventricular enlargement has not been reported in other IT ASO trials for conditions including Angelman syndrome, Dravet syndrome, *SOD1*-related ALS or *FUS*-related ALS. One possibility is that this adverse event could be a potential side effect triggered by high doses of some but not all high-dose ASOs.

Potential mechanisms by which IT delivery of an ASO might trigger ventricular enlargement or hydrocephalus are unclear, but could involve changes in CSF overproduction, decreased CSF resorption and/or alterations in ventricular compliance. Genetic forms of hydrocephalus have been identified in association with mutations that perturb neuronal stem cell development and/or ciliary function[40], but neither of these biological processes have been clearly linked to *KCNT1*. However, acquired hydrocephalus can occur as a consequence of infection, inflammation or hemorrhage[41], and some ASOs have been shown to have immunostimulatory properties. These properties appear to be hybridization independent but still can depend on the presence of

certain sequences such as the CpG motif, which strongly activates Toll-like receptor 9 (TLR9). However, empiric testing of valeriasen in human peripheral blood samples (Supplementary Fig. 3) or Bjab cells (Supplementary Fig. 4) failed to reveal significant immunostimulatory properties. Further investigation will therefore be required to understand the mechanistic basis of the adverse events observed, as well as their potential generalizability. Managing these potential risks—spacing out dosing intervals, periodic brain imaging, monitoring CSF opening pressures, structured symptom screening and clinical evaluations—may deserve consideration in designing other CNS ASO trial protocols.

Overall, these results provide pilot support for the hypothesis that inhibition of Slack function can suppress seizures in *KCNT1* EIMFS, a seriously debilitating and life-threatening pediatric disorder. At the same time, the emergence of unexpected serious adverse events points to the need for deeper mechanistic investigation, underscoring the importance of careful screening, risk assessment, and proactive clinical monitoring and management.

Online content

Any methods, additional references, Nature Portfolio reporting summaries, source data, extended data, supplementary information, acknowledgements, peer review information; details of author contributions and competing interests; and statements of data and code availability are available at https://doi.org/10.1038/s41591-026-04314-9.

References

1. Burgess, R. et al. The genetic landscape of epilepsy of infancy with migrating focal seizures. *Ann. Neurol.* **86**, 821–831 (2019).
2. Kuchenbuch, M. et al. KCNT1 epilepsy with migrating focal seizures shows a temporal sequence with poor outcome, high mortality and SUDEP. *Brain* **142**, 2996–3008 (2019).
3. Amberger, J. S., Bocchini, C. A., Scott, A. F. & Hamosh, A. OMIM.org: leveraging knowledge across phenotype–gene relationships. *Nucleic Acids Res.* **47**, D1038–D1043 (2019).
4. Barcia, G. et al. De novo gain-of-function KCNT1 channel mutations cause malignant migrating partial seizures of infancy. *Nat. Genet.* **44**, 1255–1259 (2012).
5. Borlot, F. et al. KCNT1-related epilepsy: an international multicenter cohort of 27 pediatric cases. *Epilepsia* **61**, 679–692 (2020).
6. Kaczmarek, L. K. et al. International Union of Basic and Clinical Pharmacology. C. Nomenclature and properties of calcium-activated and sodium-activated potassium channels. *Pharmacol. Rev.* **69**, 1–11 (2017).
7. Bausch, A. E. et al. The sodium-activated potassium channel Slack is required for optimal cognitive flexibility in mice. *Learn. Mem.* **22**, 323–335 (2015).
8. Quraishi, I. H. et al. An epilepsy-associated KCNT1 mutation enhances excitability of human iPSC-derived neurons by increasing Slack K_{Na} currents. *J. Neurosci.* **39**, 7438–7449 (2019).
9. Kim, G. E. et al. Human slack potassium channel mutations increase positive cooperativity between individual channels. *Cell Rep.* **9**, 1661–1672 (2014).
10. Milligan, C. J. et al. KCNT1 gain of function in 2 epilepsy phenotypes is reversed by quinidine. *Ann. Neurol.* **75**, 581–590 (2014).
11. Mikati, M. A. et al. Quinidine in the treatment of KCNT1-positive epilepsies. *Ann. Neurol.* **78**, 995–999 (2015).
12. Finkel, R. S. et al. Nusinersen versus sham control in infantile-onset spinal muscular atrophy. *N. Engl. J. Med.* **377**, 1723–1732 (2017).
13. Ziegler, A. et al. Antisense oligonucleotide therapy in an individual with KIF1A-associated neurological disorder. *Nat. Med.* **30**, 2782–2786 (2024).
14. Kim, J. et al. Patient-customized oligonucleotide therapy for a rare genetic disease. *N. Engl. J. Med.* **381**, 1644–1652 (2019).
15. Korobeynikov, V. A., Lyashchenko, A. K., Blanco-Redondo, B., Jafar-Nejad, P. & Shneider, N. A. Antisense oligonucleotide silencing of FUS expression as a therapeutic approach in amyotrophic lateral sclerosis. *Nat. Med.* **28**, 104–116 (2022).
16. Tran, H. et al. Suppression of mutant C9orf72 expression by a potent mixed backbone antisense oligonucleotide. *Nat. Med.* **28**, 117–124 (2022).
17. Burbano, L. E. et al. Antisense oligonucleotide therapy for KCNT1 encephalopathy. *JCI Insight* https://doi.org/10.1172/jci.insight.146090 (2022).
18. Crooke, S. T., Witztum, J. L., Bennett, C. F. & Baker, B. F. RNA-targeted therapeutics. *Cell Metab.* **27**, 714–739 (2018).
19. Soifer, H. S. et al. Silencing of gene expression by gymnotic delivery of antisense oligonucleotides. *Methods Mol. Biol.* **815**, 333–346 (2012).
20. Korte, S. A.-O. et al. Range of neurological signs in cynomolgus monkeys after intrathecal bolus administration of antisense oligonucleotides. *Int. J. Toxicol.* **39**, 505–509 (2020).
21. Jia, C. et al. Change of intracellular calcium level causes acute neurotoxicity by antisense oligonucleotides via CSF route. *Mol. Ther. Nucleic Acids* **31**, 182–196 (2023).
22. Moazami, M. P. et al. Quantifying and mitigating motor phenotypes induced by antisense oligonucleotides in the central nervous system. *Mol. Ther.* **32**, 4401–4417 (2024).
23. Hagedorn, P. H. et al. Acute neurotoxicity of antisense oligonucleotides after intracerebroventricular injection into mouse brain can be predicted from sequence features. *Nucleic Acid Ther.* **32**, 151–162 (2022).
24. Cornelissen, L., Donado, C., Yu, T. W. & Berde, C. B. Modified sensory testing in non-verbal patients receiving novel intrathecal therapies for neurological disorders. *Front. Neurol.* **13**, 664710 (2022).
25. Gertler, T. S. et al. Functional consequences of a KCNT1 variant associated with status dystonicus and early-onset infantile encephalopathy. *Ann. Clin. Transl. Neurol.* **6**, 1606–1615 (2019).
26. Xian, J. & Helbig, I. Guardians of the epilepsy genome. *Eur. J. Paediatr. Neurol.* **42**, A4–A6 (2023).
27. El Achkar, C. M. & Spence, S. J. Clinical characteristics of children and young adults with co-occurring autism spectrum disorder and epilepsy. *Epilepsy Behav.* **47**, 183–190 (2015).
28. Demarest, S. T. & Brooks-Kayal, A. From molecules to medicines: the dawn of targeted therapies for genetic epilepsies. *Nat. Rev. Neurol.* **14**, 735–745 (2018).
29. Hill, S. F., Jafar-Nejad, P., Rigo, F. & Meisler, M. H. Reduction of *Kcnt1* is therapeutic in mouse models of *SCN1A* and *SCN8A* epilepsy. *Front. Neurosci.* **17**, 1282201 (2023).
30. McTague, A. et al. Clinical and molecular characterization of *KCNT1*-related severe early-onset epilepsy. *Neurology* **90**, e55–e66 (2018).
31. Quraishi, I. H. et al. Impaired motor skill learning and altered seizure susceptibility in mice with loss or gain of function of the *Kcnt1* gene encoding Slack (K_{Na} 1.1) Na^+-activated K^+ channels. *Sci. Rep.* **10**, 3213 (2020).
32. Goyenvalle, A. et al. Considerations in the preclinical assessment of the safety of antisense oligonucleotides. *Nucleic Acid Ther.* **33**, 1–16 (2022).
33. Zhang, Q., Liu, Y., Xu, J., Teng, Y. & Zhang, Z. The functional properties, physiological roles, channelopathy and pharmacological characteristics of the Slack (KCNT1) channel. *Adv. Exp. Med. Biol.* **1349**, 387–400 (2021).

34. Takanashi, J. -i & Takase, N. Reader response: Evidence in focus: Nusinersen use in spinal muscular atrophy: report of the Guideline Development, Dissemination, and Implementation Subcommittee of the American Academy of Neurology. *Neurology* **93**, 464 (2019).
35. Medicines and Healthcare Products Regulatory Agency. Nusinersen (Spinraza▼): reports of communicating hydrocephalus; discuss symptoms with patients and carers and investigate urgently. *Drug Safety Update* **12**, https://www.gov.uk/drug-safety-update/nusinersen-spinraza-reports-of-communicating-hydrocephalus-discuss-symptoms-with-patients-and-carers-and-investigate-urgently (2018).
36. New warning of nusinersen-related communicating hydrocephalus. *Reactions Weekly* **1714**, 3 (2018).
37. Viscidi, E. et al. The incidence of hydrocephalus among patients with and without spinal muscular atrophy (SMA): results from a US electronic health records study. *Orphanet J. Rare Dis.* **16**, 207 (2021).
38. Tabrizi, S. J. et al. Targeting huntingtin expression in patients with Huntington's disease. *N. Engl. J. Med.* **380**, 2307–2316 (2019).
39. Stoker, T. B., Andresen, K. E. R. & Barker, R. A. Hydrocephalus complicating intrathecal antisense oligonucleotide therapy for Huntington's disease. *Mov. Disord.* **36**, 263–264 (2021).
40. Wallmeier, J., Dallmayer, M. & Omran, H. The role of cilia for hydrocephalus formation. *Am. J. Med. Genet. C. Semin. Med. Genet.* **190**, 47–56 (2022).
41. Karimy, J. K. et al. Inflammation in acquired hydrocephalus: pathogenic mechanisms and therapeutic targets. *Nat. Rev. Neurol.* **16**, 285–296 (2020).

Tojo Nakayama[1,2,17], Christelle M. El Achkar[3,17], Lisseth E. Burbano[1,4], Imran H. Quraishi[5,6], Jing Wu[6], Melody Li[4], Yutaro Asami[1,2], Sean R. Golinski[7], Emma Sherrill[1], Benjamin D. Goodlett[1], Claudio M. de Gusmao[3], Danielle A. Friedman[1], Claudia Lentucci[1], Victoria Suslovitch[1], Olivia Riccardi[1], Kamli N. W. Faour[1], Ashley Kuniholm[8], Aubrie Soucy Verran[1], Siobhan Coffman[9], Banu Ahtam[10], Boxun Zhao[1,11,12,13], Diana H. Chin[1], Renata L. DiDonato[1], Chunguang A. Hu[1], Edith Lopez[1], Sonia Hills[1], Snezana Maljevic[4], Helene Tran[14], Lynn W. Bush[1,12], Patricia Ellen Grant[10,12], Joseph R. Madsen[12,15], Richard S. Smith[7], Leonard K. Kaczmarek[6,16], Charles B. Berde[9,12] & Timothy W. Yu[1,11,12,13] ✉

[1]Division of Genetics and Genomics, Boston Children's Hospital, Boston, MA, USA. [2]Nucleotide and Peptide Drug Discovery Center, Institute of Science Tokyo, Tokyo, Japan. [3]Department of Neurology, Boston Children's Hospital, Boston, MA, USA. [4]The Florey Institute of Neuroscience and Mental Health, University of Melbourne, Melbourne, Victoria, Australia. [5]Comprehensive Epilepsy Center, Department of Neurology, Yale School of Medicine, New Haven, CT, USA. [6]Department of Pharmacology, Yale School of Medicine, New Haven, CT, USA. [7]Department of Pharmacology, Feinberg School of Medicine, Northwestern University, Chicago, IL, USA. [8]Clinical Research Operations Center, Boston Children's Hospital, Boston, MA, USA. [9]Department of Anesthesia, Critical Care, and Pain Medicine, Boston Children's Hospital, Boston, MA, USA. [10]Department of Radiology, Boston Children's Hospital, Boston, MA, USA. [11]Manton Center for Orphan Disease, Boston Children's Hospital, Boston, MA, USA. [12]Harvard Medical School, Boston, MA, USA. [13]Broad Institute of MIT and Harvard, Cambridge, MA, USA. [14]R&D Servier Institute Paris-Saclay, Saclay, France. [15]Department of Neurosurgery, Boston Children's Hospital, Boston, MA, USA. [16]Department of Cellular and Molecular Physiology, Yale School of Medicine, New Haven, CT, USA. [17]These authors contributed equally: Tojo Nakayama, Christelle M. El Achkar. ✉e-mail: Timothy.Yu@childrens.harvard.edu

Methods

Ethics statement

Studies of patient-derived cells were performed with family consent under an appropriate Boston Children's Hospital Institutional Review Board (BCH IRB)-approved protocol maintained by the Manton Center for Orphan Disease Research Gene Discovery Core. Clinical investigational studies were conducted with family consent under separate BCH IRB-approved protocols (IRB-P00035937 and IRB-P00037661), with United States Food and Drug Agency permission (IND147092), and oversight from an institutional Data Safety Monitoring Committee. No compensation was provided.

Study participants

Two female patients, each aged 2 years at enrollment, were included in this study; both carried the de novo *KCNT1* c.1421G>A (p.Arg474His) variant associated with EIMFS.

Patient 1575-01 (patient 1) was a 2-year-old girl with intractable epilepsy and global developmental delay. She was born as an apparently healthy baby girl to first-time parents. She was discharged quickly after birth, only to be rehospitalized after developing seizures on her fourth day of life. Once these began, they proved to be unrelenting, with up to several dozen per day. She was diagnosed with EIMFS based on seizure semiology and EEG features. Over the course of the next several months, she was tried with a host of antiepileptic medications, including levetiracetam, topiramate, phenobarbital, diazepam, oxcarbazepine, valproic acid, quinidine, phenytoin and vitamin B_6, all with no effect. A brain MRI was normal, showing no underlying structural trigger for her seizures. At 4 months of age, a neurogenetic panel test revealed a molecular diagnosis: a non-inherited (de novo) mutation in *KCNT1* (c.1421G>A, p.Arg474His), which is a known pathogenic variant for EIMFS.

At 28 months old, she was generally healthy but had shown very little neurological development. She was able to slightly lift her head when placed in prone position. She seemed alert to sounds, but her vision was not fully fixed and she does not track well. She had a smile-like movement at times, but it was unclear whether it was social; otherwise, she cried, was quieted by being fed or held, or slept. She did not make eye contact, roll over, reach for objects or put her hands in her mouth. She was hypotonic and had between several and 20 seizures per day. She had increased tone in her upper and lower extremities, which varied depending on state and position, sometimes suggesting dystonia.

Patient 1677-01 (patient 2) was a 2-year-old girl with a history of neonatal-onset epilepsy with intractable epilepsy and global developmental delay. Seizures began at 5 h of life and consisted of apneic spells with bicycling movements. EEG showed multifocal migrating seizures. Several antiepileptic medications were trialed, including phenobarbital, levetiracetam, pyridoxine, potassium bromide, phenytoin, cannabidiol (Epidiolex) and topiramate, with limited success. Initial EEGs showed normal background for age but multifocal seizures. Subsequent EEGs were consistent with abnormal background consistent with encephalopathy, at one point described as possibly hypsarrhythmia, although she has never had a history of spasms. Genetic testing at 5 months of age revealed a de novo mutation in *KCNT1* (c.1421G>A, p.Arg474His).

At 2 years of age, she had a severe global developmental delay. She was able to grasp objects intentionally but was unable to hold on to them. Her hands were a lot more relaxed as opposed to near-constant fisting before. She held eye contact but had difficulty tracking. She was starting to find objects in space and look at them for a few seconds. She remained hypotonic axially and had increased appendicular tone. She did not roll over completely yet. She seemed to understand simple words and commands. She had a social smile. She appeared mostly alert and in touch with her surroundings according to her parents. She had 10–15 focal tonic seizures per day, sometimes associated with desaturation. The semiology was more or less consistent and was described as head turning to one side, full body stiffening, eyes deviated to the same side as the head, at times accompanied by breath holding but no blue discoloration or O_2 drop. She tends to have clusters during her afternoon naps and can have up to 6–8 seizures per hour, all brief, lasting <1–2 min.

Control and patient-derived iPSC lines

WT iPS cell line iPS(IMR90)-4 was purchased from WiCell. Patient iPSCs were derived from patient skin fibroblasts via a 2-mm skin punch biopsy maintained in a medium containing Dulbecco's modified Eagle medium (Fisher Scientific) supplemented with 10% fetal bovine serum (FBS) (Gibco). Patient fibroblasts were reprogrammed into iPSCs by introducing the four Yamanaka factors via Sendai virus. iPSCs were characterized and maintained in mTeSR-Plus medium (StemCell Technologies). Cortical neuronal differentiation was achieved via lentiviral transduction of an inducible NGN2 cassette followed by doxycycline induction (~6 days). iPSC-derived neurons were cultured in glia-conditioned Sudhof medium supplemented with BDNF, NT3 and laminin[42].

Commercially available neuronal cell lines

Human and mouse neuroblastoma cells (BE(2)-M17, SH-SY5Y Neuro2a), were obtained from the American Type Culture Collection. Cells were maintained and passaged in medium containing Dulbecco's modified Eagle medium or minimum essential medium (Fisher Scientific) supplemented with 10% FBS (Gibco). These cells used in experiments were under passage 20.

ASOs

Gapmer ASOs using mixed phosphodiester and phosphorothioate backbones and 2′MOE-nucleotide modifications were designed to be complementary to the *KCNT1* gene and synthesized (Microsynth).

ASO screening for *KCNT1* knockdown

Initial ASO screening was conducted using lipofectamine transfection. BE(2)-M17 cells, SH-SY5Y cells, WT iPSC-derived neurons and patient iPSC-derived neurons were cultured in 24-well and 96-well plates. Cells were transiently transfected (post-differentiation day 14–21 for neurons) with ASOs using the Lipofectamine 3000 transfection reagent according to the manufacturer's protocol (Thermo Fisher Scientific). After 48–72 h, RNA was isolated and cDNA was synthesized using the TaqMan Fast Advanced Cells-to-C_T Kit, following the manufacturer's protocol (Thermo Fisher Scientific). *KCNT1* mRNA expression analysis was performed via quantitative real-time PCR (qPCR) using the QuantStudio 3 Real-Time PCR System and TaqMan probes purchased from Thermo Fisher Scientific (human *KCNT1*: Hs01063050_m1; mouse *Kcnt1*: Mm01330662_m1; rat *Kcnt1*: Rn00573091_m1). qPCR was performed under standard conditions (initial denaturation at 95 °C for 2 min, followed by 40–50 cycles of denaturation at 95 °C for 1 s and annealing and extension at 60 °C for 20 s). Beta-actin (human *ACTB*: Hs01060665_g1; mouse *Actb*: Mm00607939_s1; rat *Actb*: Rn00667869_m1) and glucuronidase beta (mouse *Gusb* Mm01197698_m1) were used as endogenous controls. Quantification of *KCNT1* mRNA expression was performed by normalizing to the endogenous control gene and vehicle-treated cells (mock transfection with water) using the delta–delta Ct method. Delta Ct = $Ct_{KCNT1} - Ct_{control\ gene}$; delta delta Ct = $Ct_{ASO} - Ct_{vehicle}$; fold change (FC) = $2^{(-delta-delta\ Ct)}$. The fold change, expressed as a percentage, served as a quantitative measurement of *KCNT1* mRNA expression. Cell extracts were analyzed for KCNT1 protein levels by immunoblotting using antibodies raised against KCNT1 (ab199654, Abcam, 1/500 dilution) and beta actin (ab6276, Abcam, 1/5,000 dilution). Blots were scanned on a Li-Cor Odyssey imager (Li-Cor). Signal intensities were quantified using Image Studio Lite (Li-Cor). Each immunoblot analysis was replicated at least three times. Following initial ASO screening via lipofectamine transfection, secondary ASO validation was used via gymnosis or free uptake[19]. ASOs

were added directly to the culture medium at concentrations ranging from 0.3 µM to 10 µM. BE(2)-M17 and SH-SY5Y cells were cultured for 2–14 days, and human iPSC-derived neurons were cultured ~14 days post-doxycycline before treatment with ASOs (1–2 weeks). After ASO treatment, RNA isolation, cDNA synthesis, qPCR, immunoblotting and data analysis were performed as described above.

Mouse strains

The *Kcnt1*$^{+/R455H}$ mouse line was generated in the C57BL/6J background using CRISPR–Cas9 genome editing at the Yale Genome Editing Center. The detailed generation and characterization of these mice have been previously described[31]. Mice were kept on a 12-h light–dark cycle. Heterozygous (*Kcnt1*$^{+/R455H}$) mice were bred to produce embryos of three genotypes: wild-type (WT/WT), heterozygous (R455H/WT) and homozygous (R455H/R455H) embryos for use in primary neuronal culture experiments.

The *Kcnt1* p.P905L knock-in mouse line was generated at the University of Adelaide, also using CRISPR–Cas9 genome editing technology, as previously described[17]. Mice were housed in temperature-controlled rooms (≈22 °C) on a 12-h dark–12-h light cycle and maintained with rodent diet and water available ad libitum. A single nucleotide variant (c.2714C>T), corresponding to the human *KCNT1* p.P924L pathogenic variant associated with EIMFS, was introduced into the mouse genome. Briefly, C57BL/6J zygotes were microinjected with sgRNA, Cas9 mRNA and a single-stranded oligonucleotide repair template containing the intended mutation. Injected embryos were transferred into pseudopregnant females, and the resulting pups were genotyped and sequence confirmed for the desired variant. The colony was maintained on the C57BL/6J background through backcrossing and subsequent intercrossing to produce WT (+/+), heterozygous (L/+) and homozygous (L/L) mice. Mice of this line were used for evaluating disease phenotypes, nucleic acid therapeutic interventions and survival outcomes.

Institutional oversight for animal studies was provided by the Institutional Animal Care and Use Committees of BCH, Yale and Charles River Laboratories.

Patch-clamp electrophysiology in human iPSC and mouse cortical neurons

Whole-cell patch-clamp recordings were performed with patch-clamp amplifiers (MultiClamp 700B; Molecular Devices) under the control of pCLAMP 11 software (Molecular Devices). Patient iPSC-derived neurons were cultured on a round cover glass in a 24-well plate. ASOs were introduced via transient transfection or gymnosis. For transfection experiments, post-differentiation day (days in vitro (DIV)) 14–21 neurons were treated with ASOs at 100 nM and were analyzed by patch-clamp assay at DIV 27–29. For gymnosis experiments, cells were treated with ASOs at 10 µM for 2 weeks, followed by patch-clamp recordings at DIV 35–42. For mouse primary cortical neuron experiments, ASOs were introduced by gymnosis on day 3, and electrophysiology experiments were conducted at DIV 15–16. Recordings were performed at physiological temperature (37 °C) or room temperature (25 °C).

Primary cortical neurons were prepared from E16–17 mouse embryos[31,43,44]. Under voltage clamp conditions, cultured mouse neurons from wild-type (WT/WT), heterozygous p.R455H (R455H/WT) and homozygous p.R455H (R455H/R455H) embryos showed increased outward K^+ currents in a genetic dosage-dependent fashion, with 2–3× and 4–6× increased currents in R455H/WT and R455H/R455H neurons, respectively, compared with the isogenic WT controls. After isolation of the cortex from embryonic brains, neurons were dissociated and seeded (on coverslips inside a 6-well plate: 0.2×10^6 cells per well) onto plates containing NB plus (Neurobasal medium supplemented with B27 (Gibco), GlutaMAX (Gibco) and penicillin–streptomycin (Gibco)) and 5% FBS (Gibco). After 2 h of incubation, primary cultures were maintained in NB plus without FBS in a 5% CO_2 and 20% O_2 incubator at 37 °C. Half of the medium was replaced on DIV 3, and the cells were treated with ASOs at a final concentration of 10 µM for 12 days.

Recording electrodes were pulled from filamented borosilicate glass pipettes (Sutter Instrument) and had tip resistances between 4 MΩ and 6 MΩ when filled with the following internal solution (in mM): 124 K-gluconate, 2 $MgCl_2$, 13.2 NaCl, 1 EGTA, 10 HEPES, 4 Mg-ATP and 0.3 Na-GTP (pH 7.3, 290–300 mOsm). The extracellular medium contained the following (in mM): 140 NaCl, 5.4 KCl, 10 HEPES, 10 glucose, 1 $MgCl_2$ and 1 $CaCl_2$ (pH 7.4, 310 mOsm), or ASCF: 125 mM NaCl, 3 mM KCl, 2.5 mM $CaCl_2$, 1.3 mM $MgSO_4$, 1.25 mM NaH_2PO_4, 26 mM $NaHCO_3$ and 13 mM glucose pH to 7.4 with NaOH, 300 mOsMo. ACSF solution was continuously oxygenated during experiments with 95% O_2 and 5% CO_2 to maintain pH 7.4. For voltage-clamp recordings, neurons were held at −80 mV to −90 mV and given 200–600-ms (to iPSC-derived neurons) or 60-ms (to primary cortical neurons) voltage pulses in 10-mV steps over a range from −90 mV or −80 mV to +50 mV or +60 mV. Current amplitudes at the end of the voltage pulse were considered to be the steady-state K^+ current. Current-clamp recordings performed on iPSC-derived neurons evaluated firing properties of neurons by injecting 200-ms square current pulses incrementing in 20-pA steps, starting at −20 pA. To compare the maximum number of APs, 1.5-s square current pulses in 20-pA steps were injected until the number of APs per stimulus reached a plateau phase. Whole-cell patch-clamp recording with patient iPSC-derived neuron analysis was independently repeated seven times at multiple institutes for validation. A subset of neurons was visualized with Alexa-Fluor-488 dye (Thermo Fisher Scientific) in a patch pipette, and Scholl analysis was performed using ImageJ v.1.53 software in a blinded fashion.

ICV ASO injections in mice

KCNT1 knockdown experiments were performed in either WT mice or PiggyBac transgenic mice expressing human *KCNT1* (generated by Cyagen). Mice (P36–P38) were anesthetized using isoflurane (Abbott Laboratories) at a concentration of 4% mixed in O_2 (vol/vol) for induction and 2% for maintenance. A subcutaneous injection of meloxicam (1 mg kg^{-1}) dissolved in 0.9% saline was given before surgery. Mice were positioned in a stereotaxic apparatus (myNeuroLab), and the scalp was cleaned with 80% ethanol. The skin was infiltrated with lignocaine (1% ampules, Pfizer) and a 1-cm incision was performed to expose the skull. A burr hole was drilled 0.8 mm lateral and 0.3 mm posterior to the bregma. The tip of a 33-G internal infusion cannula was advanced to −3.0 mm from the skull surface to reach the right lateral ventricle. The cannula was connected to a 0.5-ml glass syringe and an infusion pump (legato 210/210p syringe pump, Kd Scientific). A maximum volume of 10 µl of ASO or sterile PBS was delivered at a rate of 0.5 µl s^{-1}. The cannula was withdrawn 1 min after the infusion was completed, and the skin was closed with 4-0 polyglactin 910 absorbable sutures (coated Vycryl, Ethicon). Following surgery, the animals recovered in a Thermacage (Datesand) for 1 h, then were transferred back to their home cages and monitored. Weight was recorded before injection and at the end of the experiment. The experiments were conducted under the oversight of the Florey Institute for Neuroscience and Mental Health Animal Ethics Committee.

Mouse brain *KCNT1* mRNA analysis

Tissue was collected 10–14 days postinjection. The mice were anesthetized with 4–5% isoflurane (Abbott Laboratories) and then killed for dissection. After the brain was removed from the skull, the right cortex and left hemisphere were dissected. The left hemisphere was further dissected into four areas: frontal, parietal–temporal, occipital and cerebellum. A fragment of the thoracic spinal cord was collected using hydraulic extrusion with Ca^{2+}- and Mg^{2+}-free PBS. All dissected tissue was snap frozen in liquid nitrogen and stored at −80 °C until RNA collection. Total RNA was isolated from the right cortex using TRIzol reagent following the manufacturer's protocol (Thermo Fisher Scientific).

Contaminating genomic DNA was removed with DNase treatment using DNA-free Reagents (Thermo Fisher Scientific). For quantitative reverse transcription and polymerase chain reaction (RT-qPCR), oligo deoxythymidylic acid (oligo-dT)-primed cDNA was synthesized from the total RNA. *Actb* or *Gusb* was used as an endogenous control for quantification of mouse *Kcnt1* and human *KCNT1* (for humanized transgenic mice) mRNA expression. Relative gene expression values were obtained by normalization to an endogenous control gene with a qPCR method as described above.

Nesting assessments

Nesting assessments were conducted as previously described[17]. Briefly, mice were transferred to a behavior testing room at least 30 min before testing. Two facial tissues (18 × 18.5 cm; 1.75–1.9 g; Austwide Paper products) were deposited in the cage 2 h before the onset of the dark phase (5–6 p.m.), and the quality of the nest was graded 48 h later (scores from 0 to 5, adapted from previous studies[45]).

Human participant approvals and patient inclusion

Clinical studies were submitted as a single-center, investigator-initiated research IND with approval from the BCH Oversight Committee for Personalized Experimental Therapeutics. Inclusion and exclusion criteria are described in Supplementary Table 1. Protocols were approved by the IRB (IRB-P00035937 and IRB-P00037661) and the Federal Food and Drug Administration via an investigational new drug application (IND147092, under section 505(i) of the Federal Food, Drug, and Cosmetic Act). Ongoing monitoring was conducted by an institutional Data Safety Monitoring Committee.

In silico off-target analysis

In silico analyses for potential off-target effects were performed by a sequence search tool (GGGenome). Potential off-target hybridization to non-*KCNT1* transcripts was assessed using human mRNA (RefSeq human RNA release 90, September 2018) and pre-spliced mRNA sequences (RefSeq curated protein coding on hg38, D3G 19.06, June 2019) with different numbers of mismatches tolerated for nonspecific binding. In addition, progressively end-trimmed versions of the KT777 lead ASO sequence were generated and assessed. Alignment results were analyzed and reported with respect to the NCBI RefSeq gene annotation.

In vitro off-target analysis

Empirical analysis of off-target effects was performed in human neurons derived from the iPS(IMR90)-4 control iPS cell line (WiCell). iPSC-derived neurons were cultured in a 24-well plate, and 10 µM of KT777 (valeriasen, targeting *KCNT1*), BIIB067 (sequence equivalent to tofersen, targeting *SOD1*)[46] or HTTRx (sequence equivalent to tominersen, targeting *HTT*)[38] was introduced via gymnosis at DIV 22. Media were exchanged at DIV 23. RNA was isolated at DIV 29 using the PureLink RNA Mini Kit (Thermo Fisher Scientific).

RNA extracted from iPSC-derived neurons was sequenced using the Illumina NovaSeq platform using paired-end 150-base-pair reads to a minimum of 100 MM raw reads per sample (Novogene). Data were preprocessed and aligned to the Genome Reference Consortium Human Build 38 (GRCh38) sequence using the Spliced Transcripts Alignment to a Reference (STAR v.2.7.11) open-source software[47]. Differential gene expression analysis was performed using featureCounts[48] and DESeq2 (ref. 49) from Bioconductor v.3.20. Differentially expressed genes between ASO-treated lines and the naive control line were identified, and genes with $P_{adj} < 0.05$ were considered statistically significant (Benjamini and Hochberg and DESeq2). Differentially expressed genes between ASO-treated lines and the naive control line were identified, and genes with $P_{adj} < 0.05$ were considered statistically significant (Benjamini and Hochberg and FDR adjustment)[50]. $\log_2$(FC) shrinkage was performed using the Approximate Posterior Estimation for generalized linear model (apegl m) /FDR adjustment). $\log_2$(FC) shrinkage was performed using the approximate posterior estimation for generalized linear model (apeglm) method[51]. Gene set enrichment analysis was performed on upregulated and downregulated differentially expressed genes using clusterProfiler[52] from Bioconductor v.3.20 with Biological Process Gene Ontology annotations. The samtools v.1.21 package was used to sort bam files before alignment.

IT injections in rats

Six-week-old Sprague Dawley rats were used to evaluate the safety of lead clinical candidates as well as for validation of *Kcnt1* knockdown. Preclinical safety studies were performed with Good Manufacturing Practices-grade ASOs (ChemGenes) manufactured in accordance with draft United States Food and Drug Agency guidance for individualized ASO drug products[53].

Phase 1 safety studies involved single-dose direct IT injections of 0.2 mg, 1 mg, 2 mg and 3 mg of the test article (representing ~2×, 10× and 30× typical human doses after compartmental scaling) followed by observation out to 15 days. Outcome measures included detailed in-life clinical observations, functional observation batteries, individual body weights, and microscopic and histologic evaluation of the brain, spinal cord and site of administration. In addition, tissue was collected from the spinal cord (three levels), brain (six areas) and spleen for hybridization ELISA-based determination of drug levels.

Phase 2 safety studies were conducted using repeat IT dosing of the test article at the lumbar level via a surgically implanted catheter at 0 mg, 0.05 mg, 0.2 mg or 0.8 mg over the course of a 5-month study. Doses were delivered on days 1, 15, 29, 43 and 99, and necropsies were performed on day 115. A total of 20 rats (10 male, 10 female) were included in each dosing group. For the 0 mg and 0.2 mg repeat-dose groups, an additional 10 animals (5 male, 5 female) were included in a recovery study (following the same dosage schedule but necropsies performed on day 155). Outcome measures include in-life behavioral cage-side observations, functional observation batteries, complete gross pathological examination and microscopic evaluation of hematoxylin and eosin sections of multiple organs. In addition, tissue was collected from the spinal cord (three levels), brain (six areas) and spleen for hybridization ELISA-based determination of drug levels, RNA and protein-level analyses.

Clinical dosing and safety assessments

The starting human dose for our investigational clinical study (10 mg) was chosen based on No Observed Adverse Effect Levels from GLP rat safety studies. These calculations accounted for a rat-to-human compartmental scaling factor of ~500–1,000×, based on an estimated 80–100 ml CSF volume in a 2-year-old child[54,55], compared with an estimated 6-week-old rat CSF volume of 0.1–0.15 ml (refs. 56,57). Estimates of the rat No Observed Adverse Effect Levels were 2.0 mg (single-dose GLP study) and 0.2 mg (repeat-dose GLP study), yielding estimated initial safety margins of 10–200×.

KT777 was given by IT bolus injection through lumbar puncture, starting at 10 mg and increasing every 2 weeks up to 40 mg. After dose escalation, maintenance doses were administered every 8 weeks. This regimen generally mirrored previously reported dosing regimens used for intrathecally administered RNase H-activating ASOs[15]. Clinical safety assessments included pre- and post-dose blood draws for basic laboratory tests, serial neurological assessments including quantitative sensory testing, serial vital signs and telemetry, and an annual brain and spine MRI. Clinical endpoints included a 24-h video EEG every 8–12 weeks, daily seizure logs completed by caregivers, physical therapy evaluations and serial neuropsychological assessments.

Immunoprofiling in human blood samples

Blood cell counts and cytokine and complement levels were assayed by ELISA in supernatants from human blood samples (ID.Flow, Immuneed). Briefly, fresh human whole blood from 10 healthy donors was collected and incubated with test compounds at various concentrations. Samples

were analyzed for cytokine (IL-2, IL-6, IL-8, IFNγ and TNF at baseline and after 4 h of incubation) and complement (C3a and C5a at baseline and after 15 min of incubation) levels by ELISA.

Immunoprofiling in BJAB cells

CCL22 expression was measured in BJAB cells (ACC 757: Braunschweig, Germany) following previous protocols[58]. Cells were maintained in Roswell Park Memorial Institute 1640 medium supplemented with 20% FBS and were placed in a round-bottom 96-well dish before the indicated ASO addition by gymnosis. After 24 h of incubation, the cells were collected and the total RNA was prepared with a Cells-to-Ct kit (Thermo Fisher Scientific). Levels of *CCL22* were quantified with RT-qPCR using the following primer-probe set (forward: CGCGTGGTGAAACACTTCTA; reverse: GATCGGCACAGATCTCCTTATC; probe: TGGCGTGGTGTTGCTAACCTTCA). *ACTB* expression levels were used to normalize *CCL22* results.

Clinical outcome measures

The primary endpoint was safety. Adverse events were tabulated and graded for severity according to the Common Terminology Criteria for Adverse Events version 5.0 and their relation to the study drug. In addition to safety clinical assessments, laboratory tests and imaging, quantitative sensory testing studies were implemented to monitor potential risks of dorsal root ganglion and nerve root injury, seen at high doses in animal studies of some intrathecally administered ASOs[59]. The secondary endpoint was efficacy, measured by the reduction in seizure number and duration. This was assessed through a daily caregiver epilepsy log, as well as periodic 24-h or 48-h EEG for objective seizure counts. As an exploratory endpoint, developmental changes were evaluated by a clinical neuropsychologist and included clinical and behavioral evaluations, as well as validated batteries such as Bayley-3, Vineland-3 and PEDI-CAT. Details are provided in Supplementary Table 2, and the clinical trial protocol is available upon request.

Statistics

GraphPad Prism v.9.1.1 was used for visualization and statistical analysis. Unless otherwise indicated, one-way analysis of variance (ANOVA) by repeated measures was used. Multiple comparison correction was performed using the Dunnett statistical test.

Web resources

GGGenome (https://gggenome.dbcls.jp.en) and Gene Ontology (https://geneontology.org) were used for analyses of potential off-target impacts of ASO administration.

Reporting summary

Further information on research design is available in the Nature Portfolio Reporting Summary linked to this article.

Data availability

All data supporting the findings of this study are presented in the Article and Supplementary Information. Additional clinical source data are available on request; please contact the corresponding author to arrange an appropriate data use agreement. RNA-seq count data have been deposited in the Gene Expression Omnibus of the NCBI and are accessible through GEO Series accession number GSE297948 (https://www.ncbi.nlm.nih.gov/geo/query/acc.cgi?acc=GSE297948). Database links are Genome Reference Consortium Human Build 38 (GRCh38; https://www.ncbi.nlm.nih.gov/datasets/genome/GCF_000001405.26/) and Biological Process Gene Ontology (https://geneontology.org/). Source data are provided with this paper.

References

42. Zhang, Y. et al. Rapid single-step induction of functional neurons from human pluripotent stem cells. *Neuron* **78**, 785–798 (2013).
43. Wu, J., Quraishi, I. H., Zhang, Y., Bromwich, M. & Kaczmarek, L. K. Disease-causing Slack potassium channel mutations produce opposite effects on excitability of excitatory and inhibitory neurons. *Cell Rep.* **43**, 113904 (2024).
44. Fleming, M. R. et al. Stimulation of Slack K^+ channels alters mass at the plasma membrane by triggering dissociation of a phosphatase-regulatory complex. *Cell Rep.* **16**, 2281–2288 (2016).
45. Hess, S. E. et al. Home improvement: C57BL/6J mice given more naturalistic nesting materials build better nests. *J. Am. Assoc. Lab. Anim. Sci.* **47**, 25–31 (2008).
46. McCampbell, A. et al. Antisense oligonucleotides extend survival and reverse decrement in muscle response in ALS models. *J. Clin. Invest.* **128**, 3558–3567 (2018).
47. Dobin, A. et al. STAR: ultrafast universal RNA-seq aligner. *Bioinformatics* **29**, 15–21 (2013).
48. Liao, Y., Smyth, G. K. & Shi, W. featureCounts: an efficient general purpose program for assigning sequence reads to genomic features. *Bioinformatics* **30**, 923–930 (2014).
49. Love, M. I., Huber, W. & Anders, S. Moderated estimation of fold change and dispersion for RNA-seq data with DESeq2. *Genome Biol.* **15**, 550 (2014).
50. Benjamini, Y. & Hochberg, Y. Controlling the false discovery rate: a practical and powerful approach to multiple testing. *J. R. Stat. Soc. Ser. B* **57**, 289–300 (1995).
51. Zhu, A., Ibrahim, J. G. & Love, M. I. Heavy-tailed prior distributions for sequence count data: removing the noise and preserving large differences. *Bioinformatics* **35**, 2084–2092 (2019).
52. Yu, G., Wang, L. G., Han, Y. & He, Q. Y. clusterProfiler: an R package for comparing biological themes among gene clusters. *OMICS* **16**, 284–287 (2012).
53. FDA *IND Submissions for Individualized Antisense Oligonucleotide Drug Products for Severely Debilitating or Life-Threatening Diseases: Chemistry, Manufacturing, and Controls Recommendations, Guidance for Sponsor-Investigators* (FDA, 2021).
54. Noguchi, S. et al. FANTOM5 CAGE profiles of human and mouse samples. *Sci. Data* **4**, 170112 (2017).
55. Davson, H. & Segal, M. B. *Physiology of the CSF and Blood–Brain Barriers* (CRC Press, 1996).
56. Carlson, G. P. & Thiede, M. L. Tissue distribution, excretion, and metabolism of [14C]hydrogen cyanamide in rats. *Toxicol. Sci.* **79**, 73–79 (2004).
57. Ghersi-Egea, J. F., Babikian, A., Blondel, S. & Strazielle, N. Changes in the cerebrospinal fluid circulatory system of the developing rat: quantitative volumetric analysis and effect on blood-CSF permeability interpretation. *Fluids Barriers CNS* **12**, 8 (2015).
58. Anderson, B. A. et al. Towards next generation antisense oligonucleotides: mesylphosphoramidate modification improves therapeutic index and duration of effect of gapmer antisense oligonucleotides. *Nucleic Acids Res.* **49**, 9026–9041 (2021).
59. Kim, J. et al. A framework for individualized splice-switching oligonucleotide therapy. *Nature* **619**, 828–836 (2023).
60. Bridel, C. et al. Diagnostic value of cerebrospinal fluid neurofilament light protein in neurology: a systematic review and meta-analysis. *JAMA Neurol.* **76**, 1035–1048 (2019).

Acknowledgements

We thank those who contributed advice and expertise to this project, including D.D. Cakici, Y. Huang and M. Nguyen for assisting with iPSC maintenance; L. Cornelissen and P. Dinakar for supporting clinical studies; A. Poduri, J. Douville, L. Black, S. Goldkind, M. Pendergast, F. Bennett, K. Tyndall, C. Reed, M. Moore, S. Agrawal, A. Krieg, Z. Hughes, K. Kahlig, M. Wittman, K. Reddy and D. Bearden for helpful discussions and scientific advice. Family consent was obtained and enrollment conducted with the support of the Manton Center for Orphan Disease Research. We gratefully acknowledge the following

for their financial support for this work: Valeria Foundation; the Hsiao Family Rare Disease Fund; the BCH Translational Research Program Mooney Family Fund; the Harrington Discovery Institute, NS102239 (L.K.K.); Swebilius Foundation (I.H.Q.); Harvard Catalyst Clinical and Translational Research Center (through the National Center for Advancing Translational Sciences; 8UL1TR000170) (A.K.); the Manton Center Pilot Project Award and Rare Disease Research Fellowship (B.Z.); R00NS112604 (R.S.S.); Fostering Joint International Research JP22KK0121; Grant in Aid for Scientific Research (B) JP23H02873 and JP23K27564; AMED grant JP23ek0109677h0001 (T.N.); and AMED Researcher Development Support Grant Program (Y.A.). Finally, we are most deeply indebted to the families of our research participants for their participation, trust and partnership.

Author contributions

T.W.Y., T.N. and C.M.E. conceptualized the paper. V.S. provided consultation to patient families and enrolled patients. L.W.B. provided bioethical consultation. B.Z., A.S.V. and T.W.Y. designed and/or performed computational analysis. T.N., R.L.D., D.H.C., L.E.B., B.Z., Y.A. and T.W.Y. organized and/or performed ASO design, screening and/or in vitro validation for ASO development. I.H.Q., R.S.S., T.N., J.W., S.R.G. and L.K.K. designed and carried out patch-clamp experiments on mouse cortical neurons and iPSC-derived neurons. L.E.B., M.L., S.M., S.P. and T.W.Y. designed and conducted in vivo validation for ASO development. C.M.E., C.M.d.G., C.A.H., A.S.V., E.S., B.Z., A.K., C.L., C.B.B. and T.W.Y. designed, coordinated and/or conducted IND application-enabling studies (manufacturing, pharmacokinetics and toxicology; preparation of the IND application). C.M.E., C.M.d.G., C.A.H., S.C., A.S.V., A.K., O.R., D.A.F., K.N.W.F., E.L., S.H., B.D.G., J.R.M., C.B.B. and T.W.Y. designed, coordinated and/or conducted the clinical study. C.M.E. is the principal investigator of the IND. T.N. and H.T. designed cytokine release analyses. T.N. and T.W.Y. wrote the paper with input from all authors. L.K.K. and T.W.Y. provided project supervision. T.W.Y. coordinated the overall study.

Competing interests

T.W.Y. has served as an ad hoc scientific consultant to and/or has received speaker honoraria from Biomarin, GeneTx, Alnylam, SynaptixBio, Third Rock Ventures, Servier Pharmaceuticals and Lilly Pharmaceuticals. He is named as an inventor on three patents pertaining to ASO treatments: for transposon-associated diseases (WO2019055460A1), ataxia telangiectasia (US20230174979A1) and progranulin (US11359199B2). He also serves as a board member of the N=1 Collaborative, the Oligonucleotide Therapeutics Society and the Society for RNA Therapeutics. He is a member of the N=1 Task Force for IRDiRC and also serves as a volunteer advisor to several nonprofit rare disease foundations. H.T. is an employee of R&D Servier Institute Paris-Saclay. The other authors declare no competing interests.

Additional information

Extended data is available for this paper at https://doi.org/10.1038/s41591-026-04314-9.

Supplementary information The online version contains supplementary material available at https://doi.org/10.1038/s41591-026-04314-9.

Correspondence and requests for materials should be addressed to Timothy W. Yu.

Peer review information *Nature Medicine* thanks the anonymous reviewers for their contribution to the peer review of this work. Primary Handling Editor: Jerome Staal, in collaboration with the *Nature Medicine* team.

https://doi.org/10.1038/s41591-026-04314-9

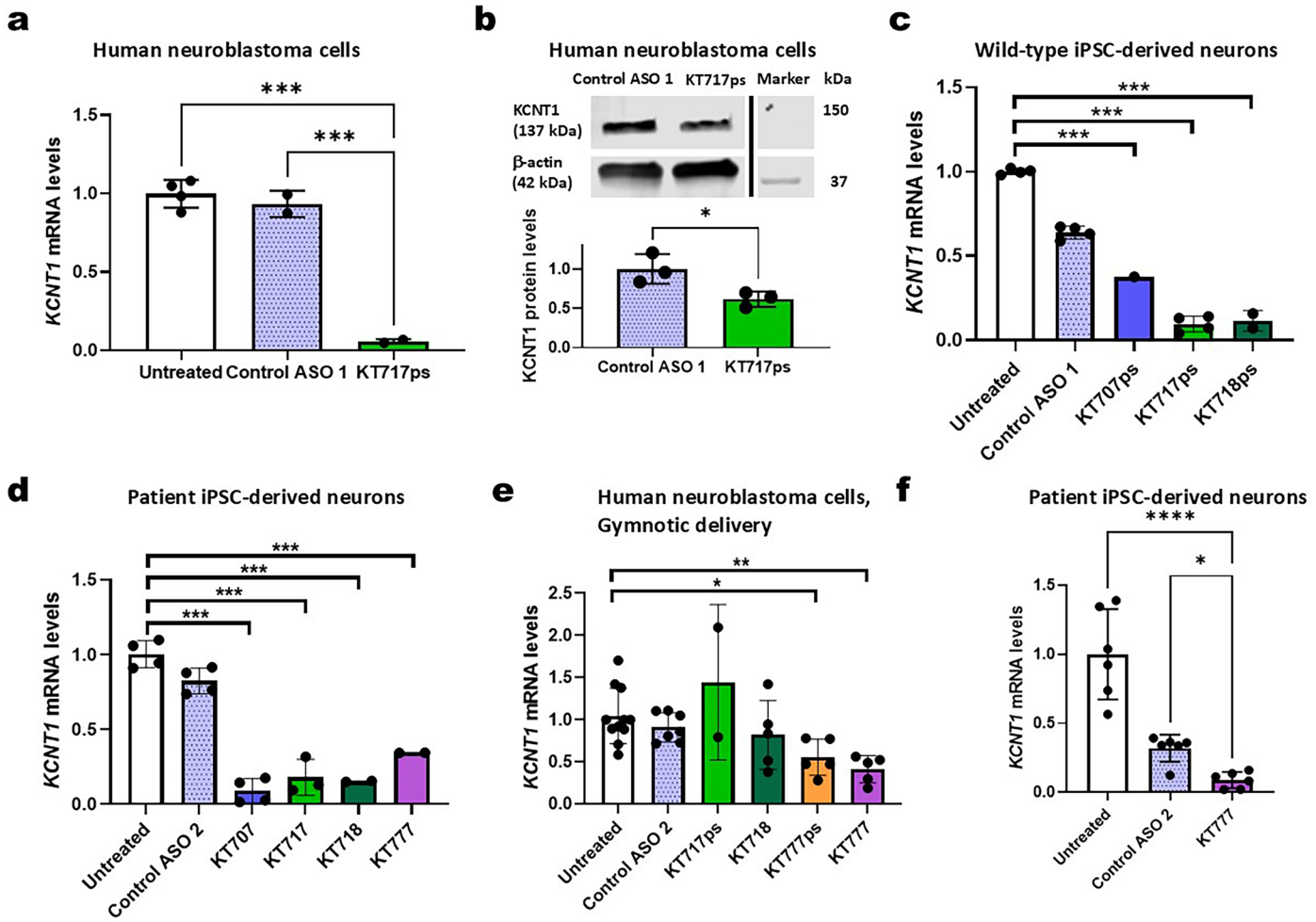

Extended Data Fig. 1 | 2′MOE-modified ASOs reduce KCNT1 mRNA transcripts in patient-derived iPSC neurons. a, **b**, Treatment of BE(2)-M17 cells with KT717ps results in significant reduction of *KCNT1* transcripts (**a**) and proteins (**b**) after 4 days incubation of 100 nM ASO via lipofection. Untreated n = 4, others n = 2, Untreated vs. KT717ps $p < 0.0001$, KT717ps vs. Control ASO 1 $p < 0.0001$ in (**a**), n = 3, $p = 0.0285$ in (**b**). **c**, Treatment of wild-type iPSC-derived neurons with *KCNT1*-targeting ASOs via lipofection (100 nM) results in significant *KCNT1* knockdown. KT707ps n = 1, KT717ps n = 4, KT718ps n = 2, others n = 4. $p < 0.0001$. **d**, Treatment of patient iPSC-derived neurons with ASOs employing mixed phosphorothioate/phosphodiester backbones via lipofection (100 nM). Untreated, Control ASO 2, KT707 n = 4, KT717 n = 3, KT718, KT777ps, KT777 n = 2. $p < 0.0001$. **e**, Treating BE(2)-M17 cells with ASOs via gymnotic delivery at 10 μM results in significant reduction of *KCNT1* mRNA levels in lead ASOs (KT777ps and KT777). Untreated n = 11, Control ASO 2 n = 7, KT777ps, KT777 n = 5, KT717ps n = 2, KT718 n = 5. Untreated vs. KT777ps $p = 0.0418$, Untreated vs. KT777 $p = 0.0054$. **f**, Treating patient iPSC-derived neurons with KT777 for one week by gymnosis at 10 μM reduces *KCNT1* mRNA levels. Control ASO 2 ps n = 5, others n = 6. Untreated vs. KT777 $p < 0.0001$, Control ASO 2 vs. KT777 $p = 0.0436$. In (**a**)-(**f**), results represent mean with SD, average of 2-3 biological replicates per experiment, 1-2 technical replicates per biological replicate. In all panels, $^{*}p < 0.05$, $^{**}p < 0.01$, and $^{***}p < 0.001$ (one-way ANOVA with Dunnett's multiple comparisons test).

https://doi.org/10.1038/s41591-026-04314-9

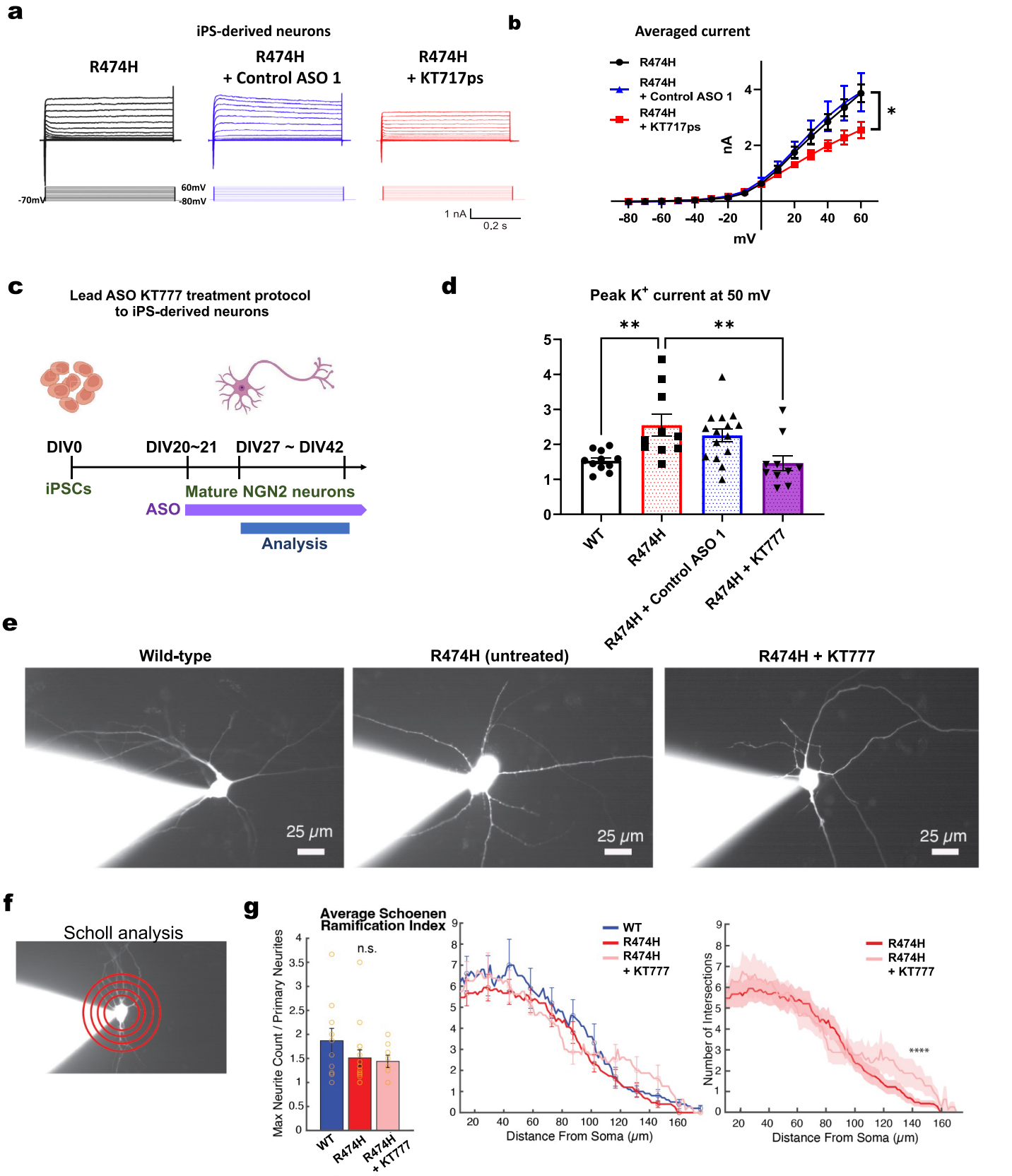

Extended Data Fig. 2 | See next page for caption.

https://doi.org/10.1038/s41591-026-04314-9

Extended Data Fig. 2 | Lead ASOs decrease K+ currents in iPS-derived neurons. **a**, **b**, Voltage-clamp recordings of iPSC-derived neurons of patient cells treated with an early developing stage lead KT717ps. Representative traces of steady-state outward currents (**a**), and averaged currents at 60 mV (**b**). Treating patient cells with KT717ps (R474H + KT717ps, red, n = 10) significantly reduced outward currents from untreated patient cells (R474H, black, n = 11) and patient cells with a control ASO (R474H + Control, blue, n = 4). The differences between the outward currents between treated and untreated cells were more evident at positive voltage steps. **c**, ASO treatment protocol to iPSC-derived neurons for the lead ASO KT777. **d**, Averaged currents of two independent experiments at 50 mV of wild-type cells (black n = 11), untreated R474H patient cells (red n = 10), R474H patient cells treated with a control ASO (blue n = 10), and R474H patient cells treated with lead ASO KT777 (purple n = 10), show a comparable pattern to a representative trace shown in Fig. 2c, confirming the consistency between experimental rounds (WT vs. R474H p = 0.0058, R474H vs. R474H + KT777 n = 0.0039). **e**, Representative images of iPSC-derived neurons. **f**, Schematic of Scholl analysis. **g**, Computational analysis of neurons through Scholl analysis demonstrates no significant difference in maximum (Max) neurite count per primary neurites (Schoenen ramification index), and a number of intersections between wild-type untreated (blue), R474H cells untreated (red), and R474H cells treated with KT777 (pink). In all panels, Data are presented as mean values ± SEM. 3 (**b** and **d**) and 2 (**e** and **g**) biological replicates per experiment. In (**b**), (**d**) and (**g**), *p < 0.05, **p < 0.01, and ***p < 0.001 (one-way ANOVA with Dunnett's multiple comparisons test). In (**g**), the multiple asterisks indicate single * significance over that range. Icons in **c** created in BioRender; Yu, T. https://biorender.com/bdozgpi (2026).

https://doi.org/10.1038/s41591-026-04314-9

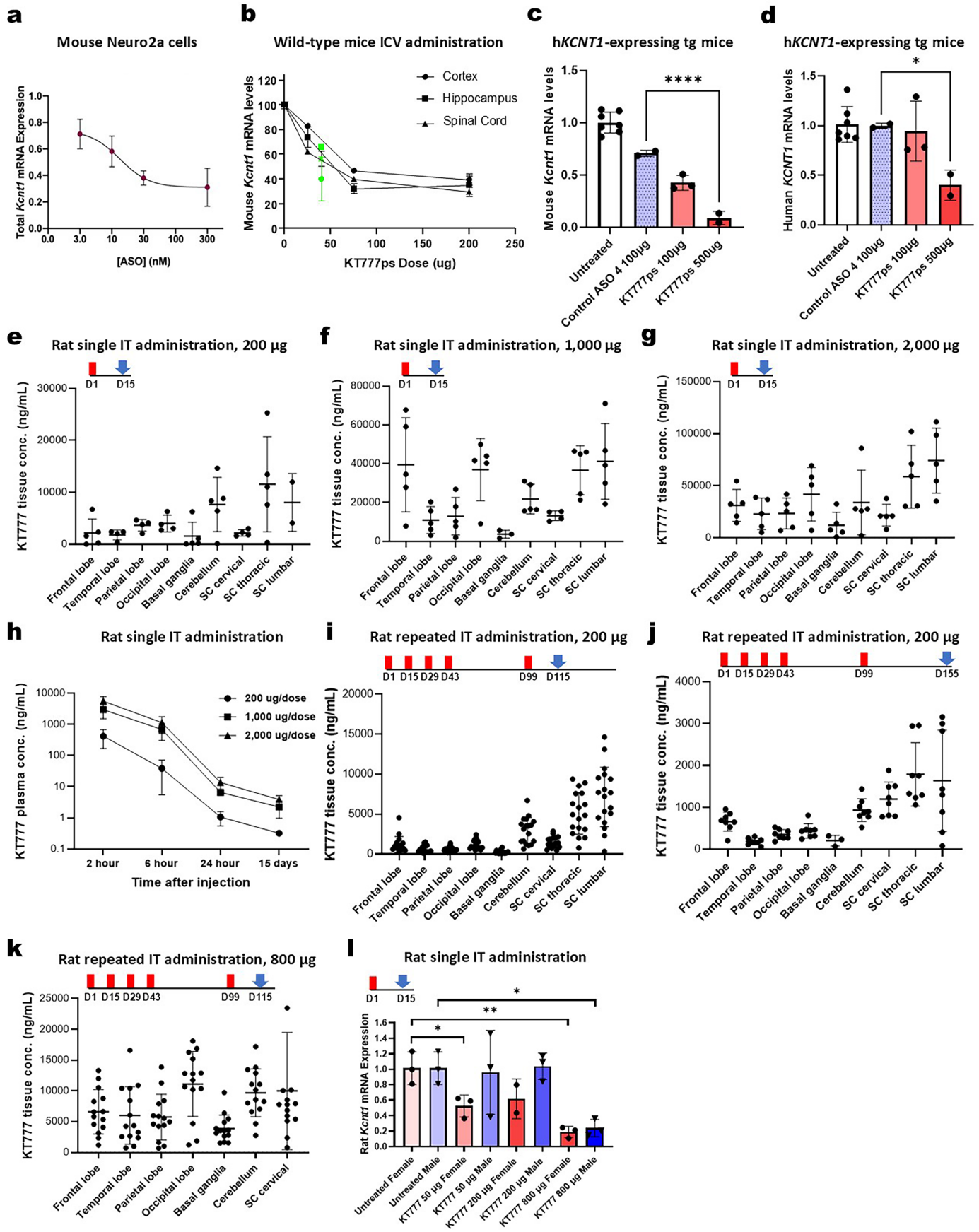

Extended Data Fig. 3 | See next page for caption.

https://doi.org/10.1038/s41591-026-04314-9

Extended Data Fig. 3 | ASO knockdown in Neuro2a cells, Kcnt1 P905L(L/L) mice, transgenic human KCNT1 mice, and wild-type rats. a, Dose-response curve of KT777ps in mouse Neuro2a cells. KT777ps was introduced at different doses via lipofection and analyzed in 2 days after treatment. n = 12 for 3 and 300 nM, n = 6 for 10 and 30 nM. **b**, Measurement of mouse *Kcnt1* levels in the cortex, hippocampus and spinal code in mice 14 days (black symbols) or 28 days (green symbols) after ICV injection with KT777ps. (n = 3, respectively). **c**, **d**, Measurement of mouse *Kcnt1* levels (**c**) or human *KCNT1* levels (**d**) in the cortex of human *KCNT1* (h*KCNT1*)-expressing transgenic mice, 10-11 days after injection with vehicle, control ASO, and KT777ps. Untreated n = 7, control ASO 100 µg n = 2, KT777ps 100 µg n = 3, 500 µg n = 3, respectively. $p < 0.0001$ in (**c**), $p = 0.0321$ in (**d**). **e-g**, Single administration of KT777 at 200 µg (**e**) 1,000 µg (**f**), and 2,000 µg (**g**) demonstrated the broad distribution of KT777 in rat brains (temporal lobe and SC cervical n = 4, SC lumber n = 2, others n = 5 in (**e**), basal ganglia n = 3, SC cervical n = 4, others n = 5 in (**f**), n = 5 in (**g**). **h**, Plasma concentration of KT777 after dosing in wild-type rats (200 µg dose 2 h and 6 h n = 5, 24 h n = 4, 15 days n = 2, 1000 µg dose n = 5, 2000 µg dose 2 h n = 4, others n = 5). **i-k**, Tissue levels of KT777 in different brain and spinal cord regions of wild-type rats receiving repeat (IT) doses of KT777 at 200 µg x5 (sacrificed on Day 115) (**i**), 200 µg x5 (sacrificed on Day 155) (**j**), or 800 µg x5 (sacrificed on Day 115) (**k**). Doses were delivered on Days 1, 15, 29, 43, and 99 (**i-k**). (**i**) n = 18, (**j**) Basal ganglia n = 3, others n = 8, (**k**) n = 14. **l**, *Kcnt1* knockdown in wild-type rat brain after repeat (50, 200, or 800 µg x5) IT administration of KT777. KT777 200 µg Female n = 2, others n = 3. Untreated Female vs. KT777 50 µg Female $p = 0.0253$, Untreated Female vs. KT777 800 µg Female $p = 0.0016$, Untreated Male vs. KT777 800 µg Male $p = 0.0378$. In all panels, Data are presented as mean values ± SEM, $^{*}p < 0.05$, $^{**}p < 0.01$, and $^{***}p < 0.001$, comparing treatment groups from samples tested by control ASOs (one-way ANOVA with Dunnett's multiple comparisons test). Injection protocols are shown at the top with dosing days (red bars) and analysis points (blue arrows).

https://doi.org/10.1038/s41591-026-04314-9

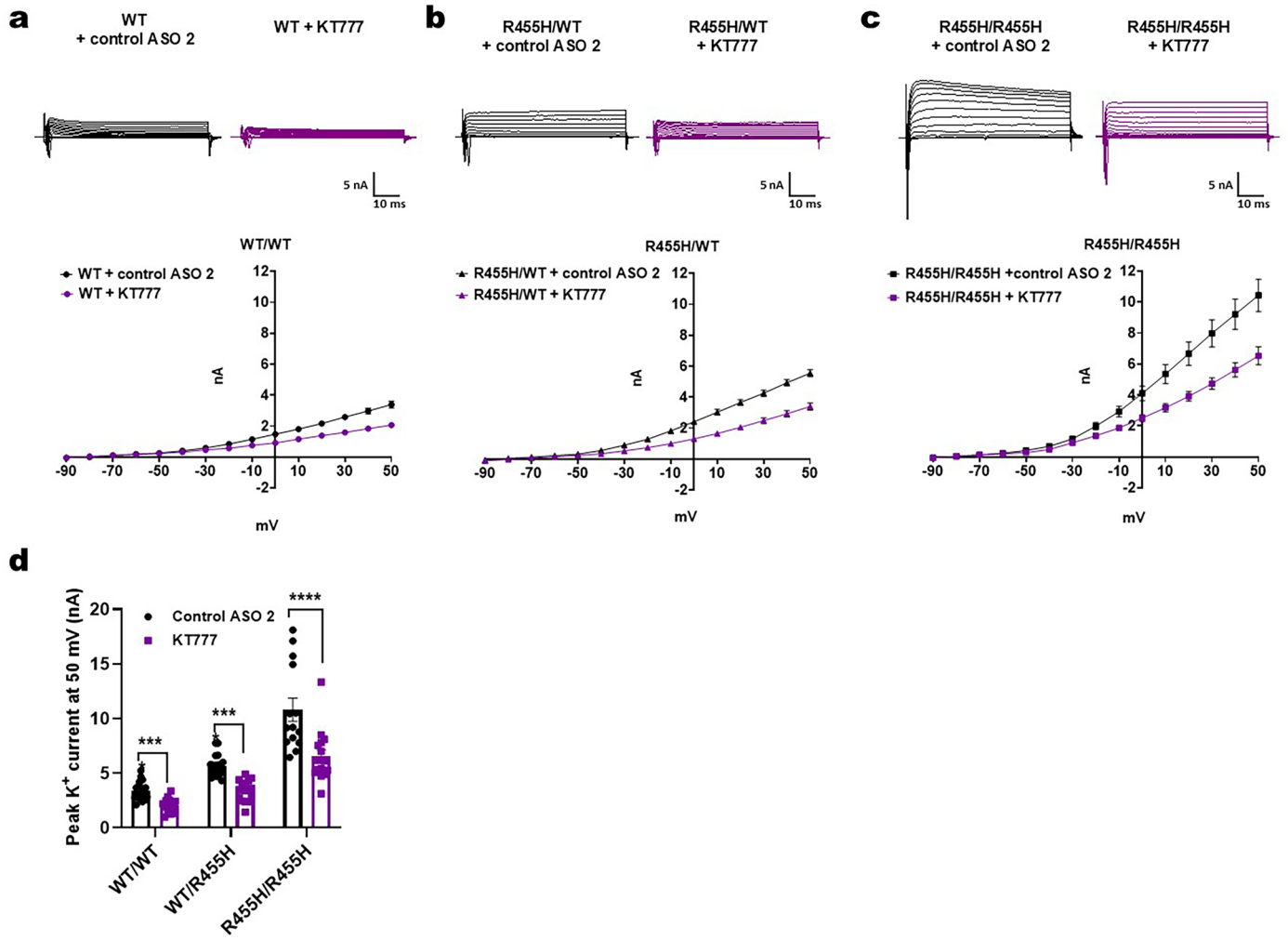

Extended Data Fig. 4 | Lead ASO KT777 suppresses K+ currents in mouse cortical neurons. a-d, Voltage-clamp recordings of wild-type and R455H mutant mouse cortical neurons treated with lead ASOs. Representative traces of steady-state outward currents, averaged currents (**a**)-(**c**) and current at 50 mV (**d**) were shown. Primary cortical neurons obtained from wild-type mice (WT/WT), heterozygous R455H mice (R455H/WT), and homozygous R455H mice (R455H/R455H) were treated with KT777, showing a significant reduction in steady-state outward current compared to the same cell types treated with control ASO. In (**a**)-(**d**), n = 15–17 neurons per condition from three independent cultures derived from three pregnant mice. Data are presented as mean values ± SEM. In all panels, *p < 0.05, **p < 0.01, ***p < 0.001, and ****p < 0.0001, (two-tailed Student's *t*-test).

https://doi.org/10.1038/s41591-026-04314-9

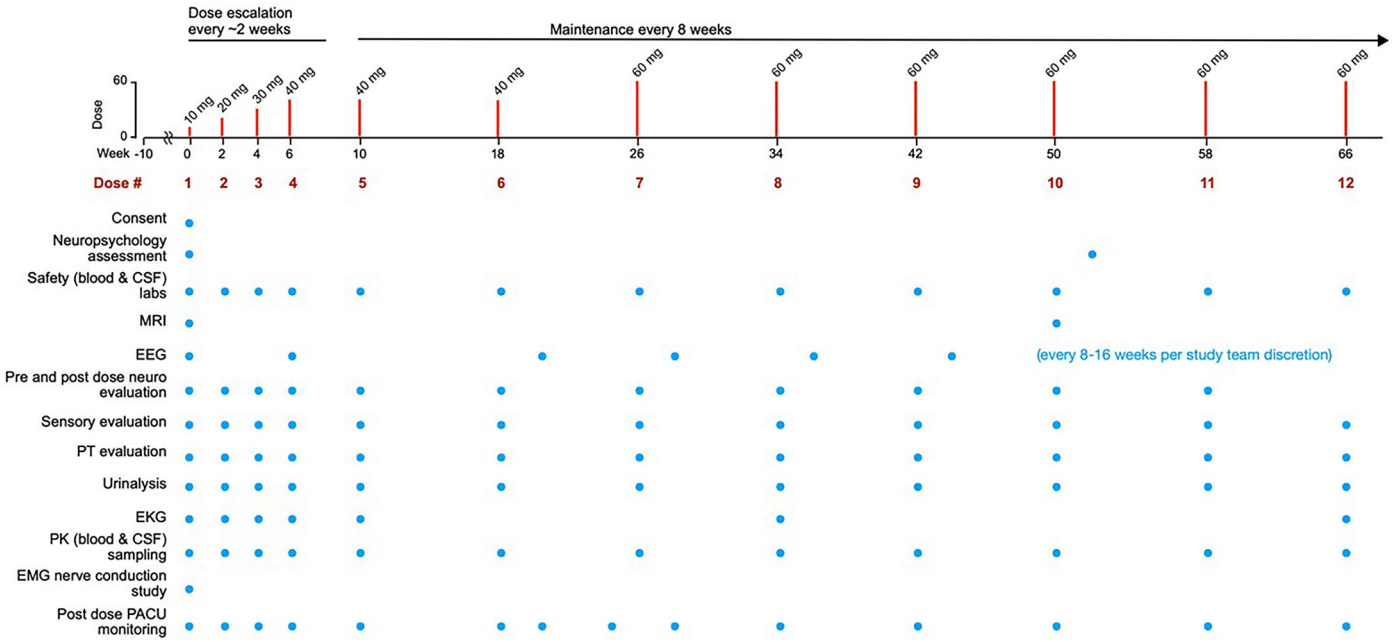

Extended Data Fig. 5 | Overview of clinical study design. Dosing schedule and schedule of assessments, with blue dots indicating timepoints for applicable assessment.

https://doi.org/10.1038/s41591-026-04314-9

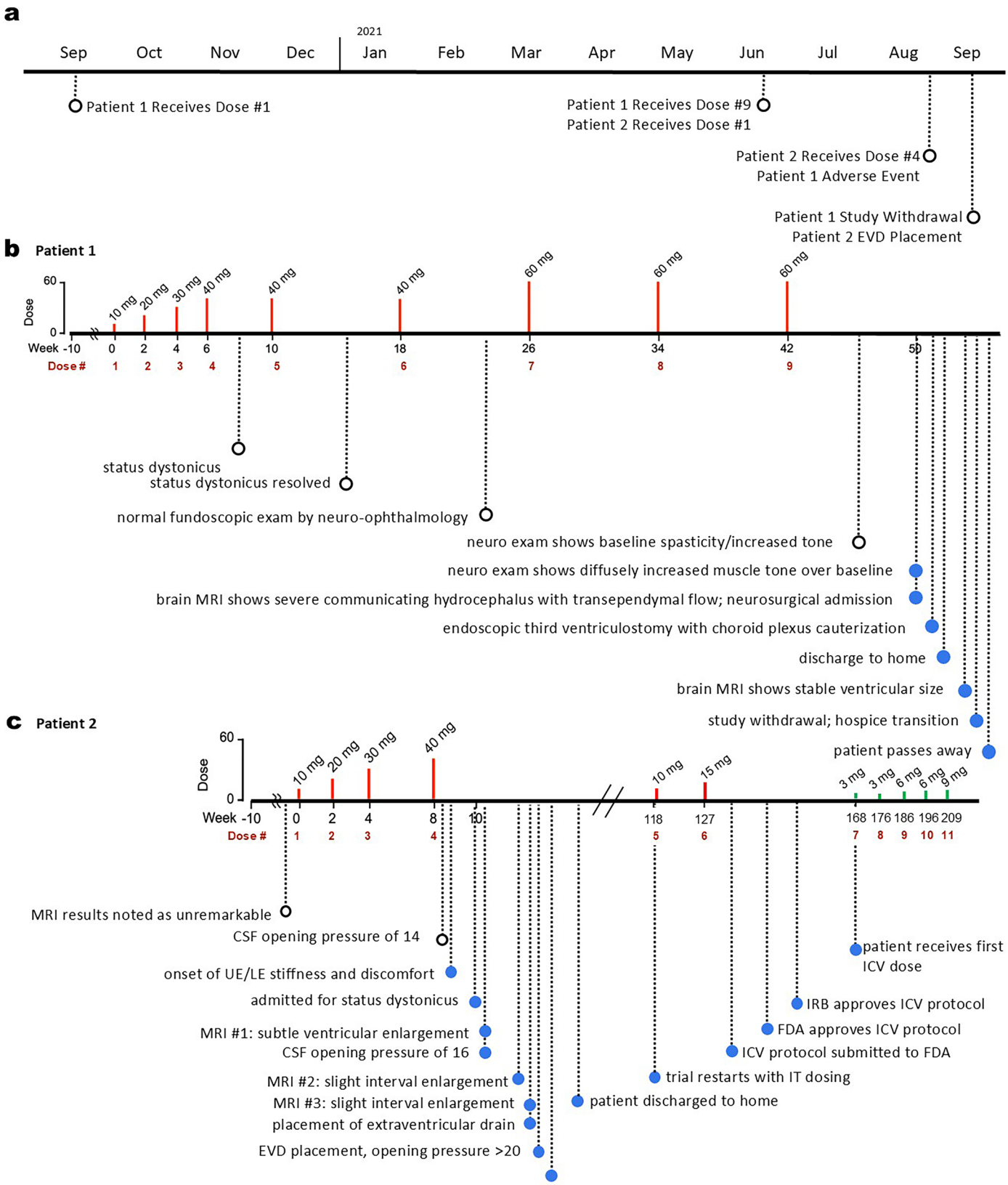

Extended Data Fig. 6 | Timeline of SAE development. a, Timeline of doses and key events for the two research participants enrolled in this study. **b, c**, Dosing schedule with detailed clinical course regarding SAE in Patient 1 (**a**) and Patient 2 (**b**). Episodes recognized as SAEs are indicated in blue circles.

https://doi.org/10.1038/s41591-026-04314-9

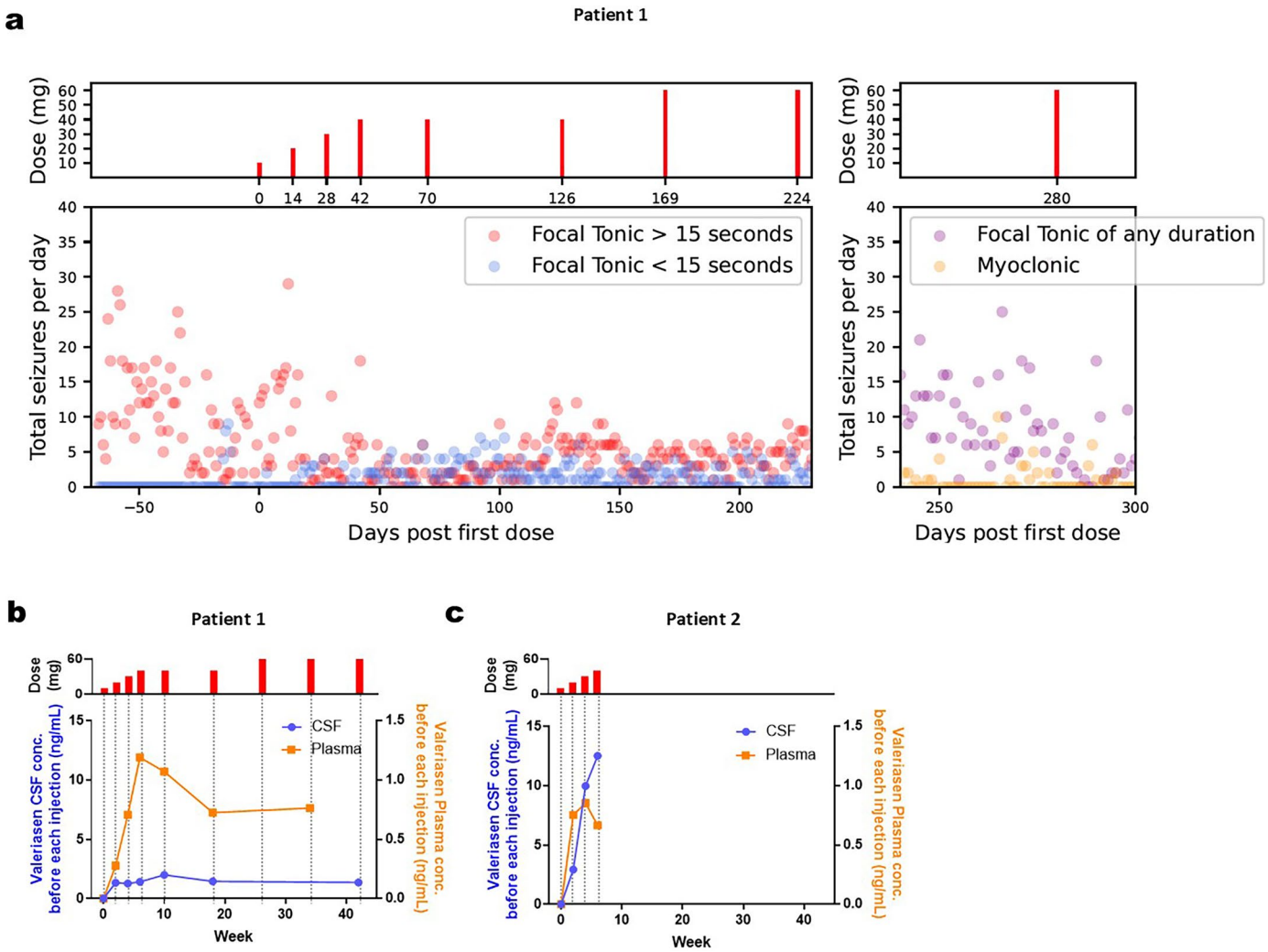

Extended Data Fig. 7 | Detailed seizure trends and valeriasen concentration. **a**, Seizure frequency and duration in Patient 1, as recorded in seizure diaries. Valeriasen dosing is indicated in red bars. Note that for Days 0-240, tonic or focal tonic seizures (with or without progression into unilateral/contralateral clonic seizures) were recorded by parents and classified by duration (lasting more or less than 15 s). After Day 240, the parental reporting schema was changed in order to capture the emergence of myoclonic seizures (subtle myoclonic movements with a duration of less than 1 second). **b**, **c**, Trough concentration of valeriasen (KT777) in cerebrospinal fluid (CSF: blue) and plasma (orange) before each administration (trough) in Patient 1 (**b**) and Patient 2 (**c**). Bars indicate the minimum and maximum values of duplicate measurements.

https://doi.org/10.1038/s41591-026-04314-9

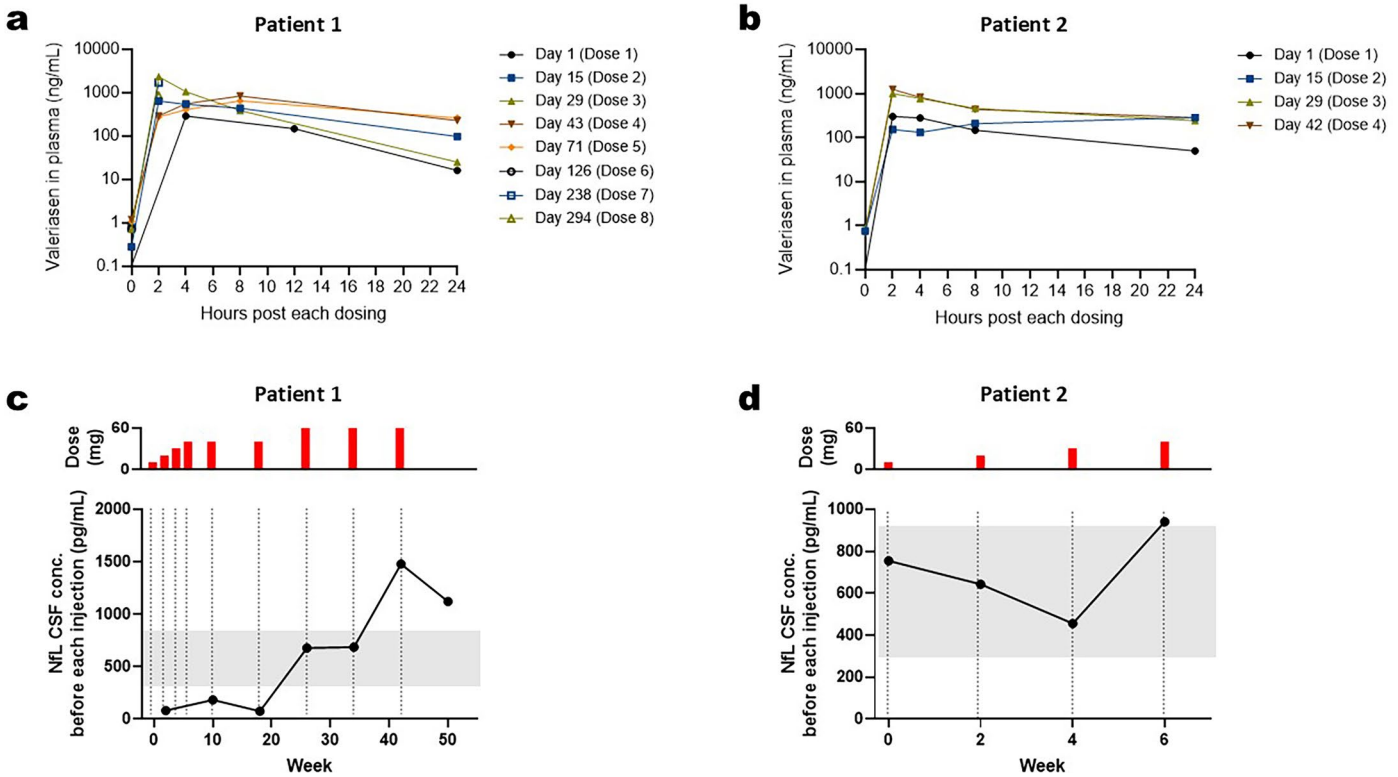

Extended Data Fig. 8 | Plasma drug levels and CSF neurofilament light chain levels in patients with EIMFS. a, **b**, Concentration of valeriasen in plasma after each administration in Patient 1 (**a**) and Patient 2 (**b**). **c**, **d**, Concentration of neurofilament light chain (NfL) in CSF prior to each administration in Patient 1 (**c**) and Patient 2 (**d**), as determined by Quanterix Simoa digital immunoassay. Shaded boxes indicate approximate interquartile reference ranges from healthy controls[60].

https://doi.org/10.1038/s41591-026-04314-9

Extended Data Table 1 | KCNT1-targeting ASO sequences used in this study

Name	Sequences and modification
KT707	**CCoCoAoG**GCGTGCAGGA**ToGoGoTC**
KT717	**CAoGoCoA**GCTGCGATGG**CoCoAoGA**
KT718	**CCoAoGoC**AGCTGCGATG**GoCoCoAG**
KT777	**GToToGoC**CTTTGTAGCT**GoAoGoGT**
KT707ps	**CCCAG**GCGTGCAGGA**TGGTC**
KT717ps	**CAGCA**GCTGCGATGG**CCAGA**
KT718ps	**CCAGC**AGCTGCGATG**GCCAG**
KT720ps	**CACCA**GCAGCTGCGA**TGGCC**
KT777ps	**GTTGC**CTTTGTAGCT**GAGGT**
Control ASO 1	**CGACTATACGCGCAATATGC**
Control ASO 2	**GCoToCoG**AATTATCCTA**GoAoGoCG**
Control ASO 3	**CCoToAoT**AGGACTATCC**AoGoGoAA**
Control ASO 4	**AToGoToG**TTCGCGTTGG**ToToAoCG**

Normal text, DNA; bold underlined text, 2′-MOE. All C residues are 5′-methyl C. All linkages are PS except where PO linkages are indicated by 'o'.

https://doi.org/10.1038/s41591-026-04314-9

Extended Data Table 2 | Off-target binding analyses for KT777 (excluding KCNT1)

	Mismatches	KT777	5' trim 1 nt	3' trim 1 nt
mRNA	0 base	0	0	0
	1 base	0	0	0
	2 bases	0	2	1
			LOXL3, OLFML2A	*RNF20*
pre-spliced mRNA	0 base	0	0	0
	1 base	0	0	0
	2 bases	0	8	6
			FUCA1, EPN2, LINC02582, LOXL3, LRP5L, WIPI2, ABCB5, OLFML2A, ZBTB20	*ANO1, HPF1, IMMP2L, SGCZ, RNF20, DCC*

The number and names of genes with potential off-target binding sites are listed.

nature portfolio

Corresponding author(s): Timothy W. Yu

Last updated by author(s): Jan 27, 2026

Reporting Summary

Nature Portfolio wishes to improve the reproducibility of the work that we publish. This form provides structure for consistency and transparency in reporting. For further information on Nature Portfolio policies, see our Editorial Policies and the Editorial Policy Checklist.

Statistics

For all statistical analyses, confirm that the following items are present in the figure legend, table legend, main text, or Methods section.

n/a	Confirmed
☐	☒ The exact sample size (*n*) for each experimental group/condition, given as a discrete number and unit of measurement
☐	☒ A statement on whether measurements were taken from distinct samples or whether the same sample was measured repeatedly
☐	☒ The statistical test(s) used AND whether they are one- or two-sided *Only common tests should be described solely by name; describe more complex techniques in the Methods section.*
☒	☐ A description of all covariates tested
☐	☒ A description of any assumptions or corrections, such as tests of normality and adjustment for multiple comparisons
☐	☒ A full description of the statistical parameters including central tendency (e.g. means) or other basic estimates (e.g. regression coefficient) AND variation (e.g. standard deviation) or associated estimates of uncertainty (e.g. confidence intervals)
☐	☒ For null hypothesis testing, the test statistic (e.g. *F*, *t*, *r*) with confidence intervals, effect sizes, degrees of freedom and *P* value noted *Give P values as exact values whenever suitable.*
☒	☐ For Bayesian analysis, information on the choice of priors and Markov chain Monte Carlo settings
☒	☐ For hierarchical and complex designs, identification of the appropriate level for tests and full reporting of outcomes
☒	☐ Estimates of effect sizes (e.g. Cohen's *d*, Pearson's *r*), indicating how they were calculated

Our web collection on statistics for biologists contains articles on many of the points above.

Software and code

Policy information about availability of computer code

Data collection	No software was used for data collection.
Data analysis	This study used the following published software tools: GGGenome, ImageJ v1.53, STAR v2.7.11, Samtools v1.21, featureCounts, DESeq2, and clusterProfiler from Bioconductor v3.20.

For manuscripts utilizing custom algorithms or software that are central to the research but not yet described in published literature, software must be made available to editors and reviewers. We strongly encourage code deposition in a community repository (e.g. GitHub). See the Nature Portfolio guidelines for submitting code & software for further information.

Data

Policy information about availability of data

All manuscripts must include a data availability statement. This statement should provide the following information, where applicable:

- Accession codes, unique identifiers, or web links for publicly available datasets
- A description of any restrictions on data availability
- For clinical datasets or third party data, please ensure that the statement adheres to our policy

All data supporting the findings of this study are presented in the main text, figures and extended figures, and supplementary content. Additional clinical source data is available on request; please contact the corresponding author (timothy.yu@childrens.harvard.edu) to arrange an appropriate data use agreement. RNA sequencing count data have been deposited in NCBI's Gene Expression Omnibus (Edgar et al., 2002) and are accessible through GEO Series accession number

GSE297948 (https://www.ncbi.nlm.nih.gov/geo/query/acc.cgi?acc=GSE297948).
Database links are, Genome Reference Consortium Human Build 38 (GRCh38) - https://www.ncbi.nlm.nih.gov/datasets/genome/GCF_000001405.26/ and Biological Process (BP) Gene Ontology - https://geneontology.org/

Research involving human participants, their data, or biological material

Policy information about studies with human participants or human data. See also policy information about sex, gender (identity/presentation), and sexual orientation and race, ethnicity and racism.

Reporting on sex and gender	Both Patient 1 and Patient 2 are reported as female.
Reporting on race, ethnicity, or other socially relevant groupings	Race and ethnicity data were not collected under this protocol. Socioeconomic status and related data were not assessed in this study.
Population characteristics	Epilepsy of Infancy with Migrating Focal Seizures (EIMFS) due to KCNT1 p.R474H mutation in two two-year-old children.
Recruitment	Patients with a confirmed KCNT1 diagnosis were referred through their parents and the disease foundation. No active recruiting occurred. The KCNT1 pR474H genotype was selected as the target of this study because it is well-studied and is known to have the most severe and reproducible impact on channel electrophysiology. Inclusion criteria for enrollment included having the p.R474H genotype, having the EIMFS clinical presentation, and being a patient at BCH. The two patients enrolled in this study were the only patients fitting these criteria.
Ethics oversight	Studies of patient-derived cells were performed with participant/family consent under an appropriate Boston Children's Hospital Institutional Review Board-approved protocol maintained by the Manton Center for Orphan Disease Research Gene Discovery Core. Clinical investigational studies were conducted with participant/family consent under separate BCH IRB-approved protocols (IRB-P00035937 and IRB-P00037661), with FDA permission (IND147092), and oversight from an institutional Data Safety Monitoring Committee. No compensation was provided.

Note that full information on the approval of the study protocol must also be provided in the manuscript.

Field-specific reporting

Please select the one below that is the best fit for your research. If you are not sure, read the appropriate sections before making your selection.

☒ Life sciences ☐ Behavioural & social sciences ☐ Ecological, evolutionary & environmental sciences

For a reference copy of the document with all sections, see nature.com/documents/nr-reporting-summary-flat.pdf

Life sciences study design

All studies must disclose on these points even when the disclosure is negative.

Sample size	Two pediatric patients with confirmed KCNT1 p.R474H mutations were enrolled in this N-of-1 study. Formal power calculations were not employed. Instead, a sample size of two was selected on the basis of the availability of patients that met the inclusion criteria, as well as ethical considerations pertaining to the appropriate number of patients to expose to a novel first-in-human drug trial.
Data exclusions	No patient data or experimental measurements were excluded from analysis.
Replication	Key safety and pharmacokinetic assessments in rodent IND-enabling studies were conducted in two independent cohorts. Gene knockdown and electrophysiology studies were replicated by independent laboratories at BCH, Yale and Northwestern.
Randomization	For human participants, this study is an N-of-1 study targeting a rare pediatric disease and therefore random allocation is not applicable. For the rodent study, mice and rats were randomly allocated to groups.
Blinding	In rodent safety studies, histopathological evaluation was conducted by a veterinary pathologist blinded to dosing group. In patients studies, there was no group allocation given the N-of-1 nature of this study.

Reporting for specific materials, systems and methods

We require information from authors about some types of materials, experimental systems and methods used in many studies. Here, indicate whether each material, system or method listed is relevant to your study. If you are not sure if a list item applies to your research, read the appropriate section before selecting a response.

Materials & experimental systems

n/a	Involved in the study
☐	☒ Antibodies
☐	☒ Eukaryotic cell lines
☒	☐ Palaeontology and archaeology
☐	☒ Animals and other organisms
☐	☒ Clinical data
☒	☐ Dual use research of concern
☒	☐ Plants

Methods

n/a	Involved in the study
☒	☐ ChIP-seq
☒	☐ Flow cytometry
☒	☐ MRI-based neuroimaging

Antibodies

Antibodies used	Anti-KCNT1 (Abcam, cat. no. ab199654), Anti-β-actin (Abcam, cat. no. ab6276).
Validation	Anti-KCNT1: WB, IP, https://www.abcam.com/kcnt1-antibody-ab199654, anti-β-actin:WB, ELISA, IHC-P, ICC/IF, FC,ChIP, Co-IP https://www.abcam.com/beta-actin-antibody-ac-15-ab6276.

Eukaryotic cell lines

Policy information about cell lines and Sex and Gender in Research

Cell line source(s)	Skin fibroblasts from two patients and their family members (established from skin biopsy samples). Human neuroblastoma cells (BE(2)-M17 and SH-SY5Y) and Mouse neuroblastome cells (Neuro2a) were purchased by ATCC.
Authentication	The patient-specific mutations were confirmed in the patient lines. The neuroloblastoma cells were not authenticated.
Mycoplasma contamination	The cell lines were not tested for mycoplasma contamination.
Commonly misidentified lines (See ICLAC register)	No commonly misidentified cell lines were used in the study.

Animals and other research organisms

Policy information about studies involving animals; ARRIVE guidelines recommended for reporting animal research, and Sex and Gender in Research

Laboratory animals	Sprague–Dawley rats (6 weeks old) and Kcnt1 P905L(L/L) transgenic mice (4-5 , 6-7 and 22-24 weeks old), as well as wild-type C57BL/6J mice (5-6 weeks old).
Wild animals	No wild-caught or non-laboratory species were used.
Reporting on sex	Both male and female mice and rats were included in studies.
Field-collected samples	No field collected samples were used in this study.
Ethics oversight	Institutional oversight for animal studies was provided by Institutional Animal Care and Use Committees of BCH, Yale, and Charles River Laboratories.

Note that full information on the approval of the study protocol must also be provided in the manuscript.

Clinical data

Policy information about clinical studies

All manuscripts should comply with the ICMJE guidelines for publication of clinical research and a completed CONSORT checklist must be included with all submissions.

Clinical trial registration	Conducted under FDA IND147092. This individual N-of-1 application is not registered or, consistent.
Study protocol	A detailed protocol (v2.1, dated 2020-08-15) defined dosing, safety monitoring, and efficacy assessments.
Data collection	The n-of-1 clinical trial has been conducted at Boston Children's Hospital since January 2020 till now.
Outcomes	Percent reduction in monthly seizure frequency compared to 50-days pre-treatment baseline.

Plants

Seed stocks	No plant samples were used.
Novel plant genotypes	No plant samples were used.
Authentication	No plant samples were used.